ISTANBUL TECHNICAL UNIVERSITY ★ GRADUATE SCHOOL

THE FRAGILITY CURVES FOR LOW-RISE REINFORCED CONCRETE BUILDINGS IN LIBYA

M.Sc. THESIS

Majdi Abu Zeyan

Department of Civil Engineering

Structure Engineering Programme

JUNE 2023

ISTANBUL TECHNICAL UNIVERSITY ★ GRADUATE SCHOOL

THE FRAGILITY CURVES FOR LOW-RISE REINFORCED CONCRETE BUILDINGS IN LIBYA

M.Sc. THESIS

Majdi ABU ZEYAN
(501191085)

Department of Civil Engineering

Structure Engineering Programme

Thesis Advisor: Prof. Dr. Hale ERGÜN

JUNE 2023

ISTANBUL TEKNİK ÜNİVERSİTESİ ★ LİSANSÜSTÜ EĞİTİM ENSTİTÜSÜ

LİBYA'DAKİ AZ KATLI BETONARME BİNALAR İÇİN KIRILGANLIK EĞRİLERİ

YÜKSEK LİSANS TEZİ

Majdi ABU ZEYAN
(501191085)

İnşaat Mühendisliği Anabilim Dalı

Yapı Mühendisliği Programı

Tez Danışmanı: Prof. Dr. Hale ERGÜN

HAZIRAN 2023

Majdi Abu Zeyan, a M.Sc student of İTU Graduate School student ID 501191085, successfully defended the thesis/dissertation entitled "**The Fragility Curves for Low-rise Reinforced Concrete Buildings in Libya**", which he prepared after fulfilling the requirements specified in the associated legislations, before the jury whose signatures are below.

Thesis Advisor : **Assist.Prof.Dr. Hale ERGÜN** ....
Istanbul Technical University

Jury Members : **Assoc. Prof. Dr. Barlas Özden ÇAĞLAYAN** ....
Istanbul Technical University

Prof. Dr. Fatma İlknur KARA ....
Gebze Technical University

Date of Submission : 26 May 2023
Date of Defense : 19 June 2023

To my wife ,To the soul of my father.

FOREWORD

I would like to express my deep appreciation and thanks for my advisors, Prof. Dr. Yasin Fahjan and Assist. Prof. Dr. Hale Ergün, for their patience and their knowledge that they have shared with me. I am grateful to all constructors and engineers back in Libya for all informations they gave to make this work possible.

Special thanks for my wife for all her supports and kinds, whome I deidcate this work for.

July 2023

Majdi Abu Zeyan
Civil Engineer

TABLE OF CONTENTS:

ABBREVIATIONS

ADRS : Acceleration-Displacement Response Spectra
DRS : Displacement Response Spectrum
FEMA : Federal Emergency Management Agency
HC : High-Code
HS : Special High-Code
LC : Low-Code
LS : Special Low-Code
MC : Moderate-Code
MS : Special Moderate-Code
NEHRP : National Earthquake Hazards Reduction Program
PC : Pre-Code
PEH : Potential Earthquake Hazards
PGA : peak ground acceleration
PGD : Permanent Ground Deformation

LIST OF TABLES

Page

LIST OF FIGURES

Page

THE FRAGILITY CURVES FOR LOW-RISE REINFORCED CONCRETE BUILDINGS IN LIBYA

SUMMARY

In the last century with the huge development in building materials, people used reinforced concrete to provide strong buildings for themselves. These buildings can stand against nature phenomena such as winds, rain, snow, etc. For the effect of earthquakes, these buildings must be considered during design to tolerate collapse and avoid damage and lives.

This study uses a new technique to develop a method that can measure the percentage of damage under earthquake motion. Using nonlinear analysis for target buildings and generating push-over curves for these houses to generate earthquake-based fragility curve. Moreover, the calculated fragility curve can help to evaluate these buildings by estimating the percentage of damage caused by a certain level of the earthquake, which leads also to help the designers to review the way to enhance the seismic performance of these buildings, as well as adding new parameters in future building code for design taking into consideration earthquake affect.

The first chapter discusses the background and scope of the earthquake history in Libya over the years. This chapter define the region of Libya seismically and describe its activity regarding earthquakes. In addition to that, some of these earthquakes caused damage to the region through loss of lives or properties. This information represents the importance of this study.

In the second chapter, the style of the buildings in Libya is shown including materials that have been developed over the years. In this chapter, it is necessary to know the type of structures that will be exposed to the effects of earthquakes when they occur.

In the third chapter, the methodology of measuring the fragility curve and estimating damage is described. Definition of FEMA HAZUS loss estimation methodology for calculating the fragility curve, and the different levels of damage. The calculation of the fragility curve depends on push-over analysis results which are calculated using software SAP2000.

In the fourth chapter, the description of this study case's building is given. The dimensions and properties, as well as the number of stories and the definition of loads. In this study, two types of buildings are primarily used by locals in Libya for residential buildings. To determine a push over or capacity curve for the case study building, we model the two buildings and define loads, hinges, and materials' details. After calculating the capacity curve, using FEMA HAZUS loss estimation

methodology to generate the estimated fragility curve based on the damage percentage of the building related to corresponding drifts.

The performance point can be calculated at the intersection of capacity curve and demand curve for the common maximum earthquake in the region given by the spectral acceleration. Using the calculated spectral displacement at the performance point caused by the maximum earthquake in a region, we can estimate the percentage of damage to the building.

LİBYA'DAKİ AZ KATLI BETONARME BİNALAR İÇİN KIRILGANLIK EĞRİLERİ

ÖZET

Son yüzyılda inşaat malzemelerindeki büyük gelişme ile insanlar kendileri için sağlam yapılar yapılmasını sağlacak şekildebetonarme kullanmışlardır. Bu yapılar, rüzgar, yağmur, kar, vb. doğal olaylarına karşı dayanıklıdırlar. Deprem etkisi için, bu evlerin yıkılmayı tolere edecek ve daha sonra hasar görmesini ve can kaybını önleyecek şekilde tasarlanması dikkate alınmalıdır.

Bu çalışmada, depremin çoklu değerleri altında farklı seviyelerde hasar yüzdesini ölçebileceğimiz bir yöntem geliştirmek için yeni bir teknik kullanılmıştır. Bu yöntem, hedef evler için doğrusal olmayan analiz kullanılarak oluşturulabilen ve bu evler için itme eğrisini oluşturan kırılganlık eğrisi olarak adlandırılır. Ayrıca, hesaplanan kırılganlık eğrisi, depremin belirli bir seviyesinden kaynaklanan hasar yüzdesini tahmin ederek bu evlerin değerlendirilmesine yardımcı olabilir; deprem etkisi dikkate alınarak tasarım için yeni konut yönetmeliğine yeni parametreler eklenmesi sağlanabilir.

Birinci bölümde, geçmiş yıllarda Libya'da meydana gelen ve sıkışıp kalan deprem tarihi, kapsamı ve arka planı hakkında bilgi verilmiştir. Bu bölüm, Libya bölgesi sismatik olarak tanımmış ve depremler açısından ne kadar aktif olduğunu daha fazla detaylandırılmıştır. Buna ek olarak, bu depremlerin bir kısmı bölgede can veya mal kaybı olarak önemli hasarlar bırakmıştır. Bu bilgi, bu çalışma için çok önemli bir ihtiyacı temsil etmektedir.

İkinci bölümde, yıllar içinde geliştirilen malzemeler de dahil olmak üzere Libya'da var olan binaların tarzı gösterilmektedir. Bu bölümde, meydana geldiğinde deprem hasarlarına maruz kalacak yapı tiplerinin bilinmesi gerekmektedir.

Üçüncü bölümde, kırılganlık eğrisinin hesaplanması ve hasar tahmininin metodolojisi açıklanmıştır. Kırılganlık eğrisini ve farklı hasar seviyelerini hesaplamak için hazus tanımı ve kodu. Kırılganlık eğrisinin hesaplanması, SAP2000 yazılımı kullanılarak hesaplanan itme analizi sonucuna bağlıdır.

Dördüncü bölümde, bu çalışmada kullanılan yapı örneği tanımlanmaktadır. Yüklerin tanımı ile birlikte katların boyutları ve özellikleri ile kat sayısı. Bu çalışmada, Libya'da yerel halk tarafından çoğunlukla konut amaçlı kullanılan iki tip bina ele alınmıştır. Bu iki binayı modelledikten ve yükleri, mafsalları ve malzeme ayrıntılarını tanımladıktan sonra, örnek olay binası için itme veya kapasite eğrisini bulmak için doğrusal olmayan analiz çalıştırılmıştır. Kapasite eğrisini hesapladıktan sonra, hazus kodunu kullanarak, meydana gelen yer değiştirmeyle ilgili binanın hasar yüzdesine dayalı olarak tahmini kırılganlık eğrisi çizilmiştir.

Son bölümde, spektral ivmede verilen bölgede yaygın olarak meydana gelen olağan maksimum deprem için, kapasite eğrisi ile talep eğrisinin kesiştiği noktada performans

noktasını biliyoruz. Bölgedeki maksimum depremin neden olduğu hesaplanan maksimum yer değiştirme kullanılarak, bina için hasar yüzdesi tahmin edilebilir.

1. INTRODUCTION

1.1 General

Humanity suffers from earthquakes in severe ways, resulting in thousands of deaths and injuries. People need to have a home that provides safety and is safe from collapsing after an earthquake strikes. The earthquake that occurred in Turkey and Syria at the beginning of 2023 caused thousands of deaths and injuries. It is necessary to develop the building design with materials to avoid such catastrophes. Therefore, studies about the design of house buildings and other buildings must be taken seriously by researchers to shed light on safety during earthquakes. For those existing buildings that have been built with no seismic consideration, studies shall be conducted to evaluate their resistance and stability, and also to estimate the level of damage that does not put people’s lives in danger.

1.2 The Purpose of The Thesis

Due to the growth of the population in Libya, as well as the availability of spacious land, locals should build their houses to raise children and settle down. The type of residential buildings can take many forms, but the most common are those built with reinforced concrete. As a result, these buildings must be designed to withstand a variety of natural phenomena, such as winds, earthquakes, etc. The parameter factor is the percentage of damage that is expected, therefore here comes the importance of the fragility curve to measure and give probability of the damage for certain buildings and different earthquake and soil types. Some studies were published about fragilty curve for existing building in the area around Libya but no previous study were found in Libya. This work is the first such work about fragilty curves, although a number of papers were published relative on other subjects linked to seismicity in Libya.

1.3 Objective and Scope of The Study:

This thesis analyzes two residential buildings with two floors each in a part of Libya which is Misurata city. These two buildings represent the usual types of houses locals build. We model two existing building using SAP 2000 software. After analyzing and obtaining the capacity curve for models using the pushover method, the fragility curve can be derived by applying the FEMA hazus methodology. The fragility curve will help to estimate the damage levels of these buildings under different earthquake grades.

1.4 Outline of The Thesis:

This study has five chapters. Chapter 1 presents a brief siesmic background in Libya. The data of past earthquake with significant magnitute are presented in this chapter along with one of most remarked earthquake occured in present era. Chapter 2 presents brief architecture style of building in Libya for different times. Chapter 3 presents the methodology of thesis calculations. It covers the method of HAZUS to find and draw the fragility curve. Also it covers the capacity curves for the buildings as well as the target displacement based on the demand spectrum. Chapter 4 covers the modeling of the two buldings and the definistion of materials proparties and load combinations. In this chapter, the results of analysis are shown and presented which are used for drawing the fragility curve. In Chapter 5 covers the discussion of the results and the spectrum for Misurata and the target displacement for study case buildings. Last chapter is the conclusion of this study with notes and results as well as any requires for future such study.

2. LIBYAN EARTHQUAKE ARCHIVE

2.1 Background of Libya's Seismicity

In Libya, seismic activities have been deemed minor, yet several quakes with a magnitude of 5.0 or higher have been documented in various regions of the country. Its seismic past has not been as damaging as in other places. However, several earthquakes of up to 7 on the Richter scale occurred on April 19, 1935. This is believed to be the strongest earthquake event in Libya and one of the most significant earthquakes in Africa.

The region located at the Mediterranean border of the African Shield has a particularly captivating seismic activity history, both in ancient and contemporary eras. The intricate geological formations situated between Eurasia and Africa, combined with the movement of the tectonic plates along with the forces causing them to do so, produce considerable variations in seismic activity in the region. Libya is highly susceptible to seismic activity. It is situated in the Mediterranean foreland at the north-central edge of Africa, and has experienced a lot of earthquake activity, especially along its northern coast. To gain insight into seismic activity in this tectonic setting, data from instrumental records must be relied upon as many historical earthquakes remain unknown or unrecorded. It is crucial to identify the hazards and history of ancient and modern earthquakes in order to estimate the risk of death, injury, and economic losses from future earthquakes.

2.2 The History of Earthquakes in Libya

As a result, an archive was created which includes data from the Classical period (262 AD) to the present day as shown in (figure 2.1).

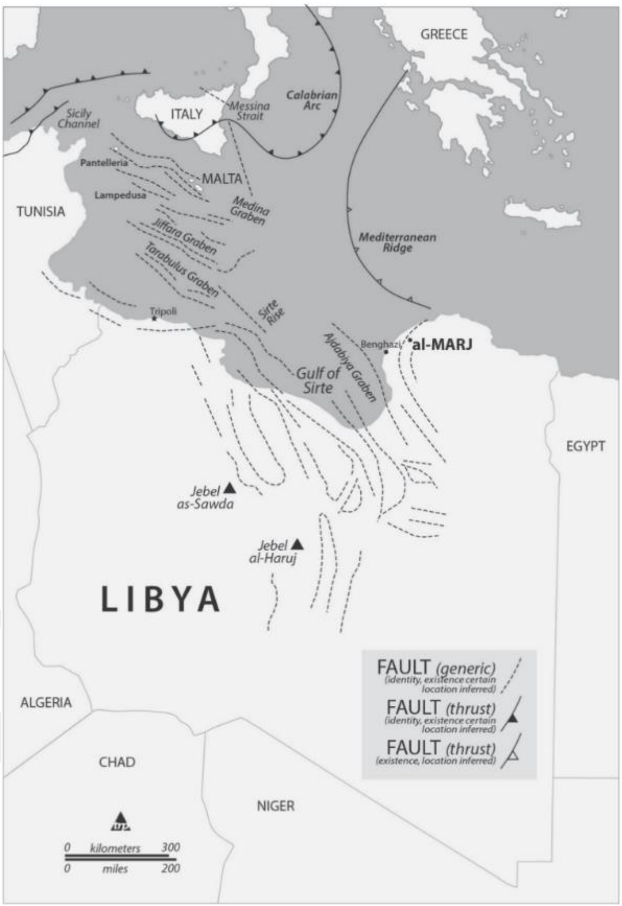

Figure 2.1: Tectonic map of Central Mediterranean Sea and Tripolitania-Sirte Basin, Libya. (Somaia S. Suwihli,2020)

By using historic documents and archaeological data, researchers compiled a record of past and ancient earthquakes for which there was no existing documentation. As there was no seismological data from that time, the archive was mostly based on archaeological evidence. Digging up and figuring out how old artifacts connected to wreckage and structural collapse have been used a lot and proven to be reliable. This is when records match earthquake dates and estimated strength and size.

The first officially recorded earthquake in Libya dates back to 262 A.D., as documented in the Historia Augusta. This was around the same time Gallienus and Faustinus were consuls. This quake had a huge impact on all of Cyrenaica, with Cyrene receiving the largest damage; the ruins are still visible today. This study divided seismic events from 262 A.D. through 1900 into two groups, based on the availability of new technologies which enabled more accurate event records (Ambraseys, N.N., 1984).

Table 2.1 : Historic earthquakes affecting Libya, up to 1900 (Ambraseys, N.N. ,1984).

Date A. D. Year m: d:	Level of Effects	Location Lat ˚N Long ˚E	Magnitude (Descriptive)	Location and Remarks
262	Damage	E. Mediterranean	Large	Cyrene and other cities destroyed in the Cyrenaica region
306 to 310	Damage	N. Libya	Large	Sabratha
365	Damage	N. Libya		Sabratha
365 7 21	Damage	E. Mediterranean		Cyrenaica
704		S.W. Libya	Large	Towns and villages in Fezzan and Sebha destroyed
1183	Damage	N.W Libya	Large	Tripoli destroyed, 20,000 deaths
1656	Damage	N.W Libya	Large	Tripoli half houses destroyed
1685 5 25	Damage	N.W Libya	Large	Tripoli, >200 buildings collapsed
1803	Felt	N.W Libya	Small	Tripoli
1811	Felt	Libya-Egypt border	Large	Siwa Temple Ammon damaged
1853 8 5 1853 10 11	Felt	S.W Libya	Small	Murzuq
1870 6 24	Felt	N. Libya	Small	Benghaz
1881 6 10	Felt	Libya-Tunisia border	Small	Eastern Tunisia, between Gabes and Meret
1883 8	Damage	W. Libya	Small	Ghadamis

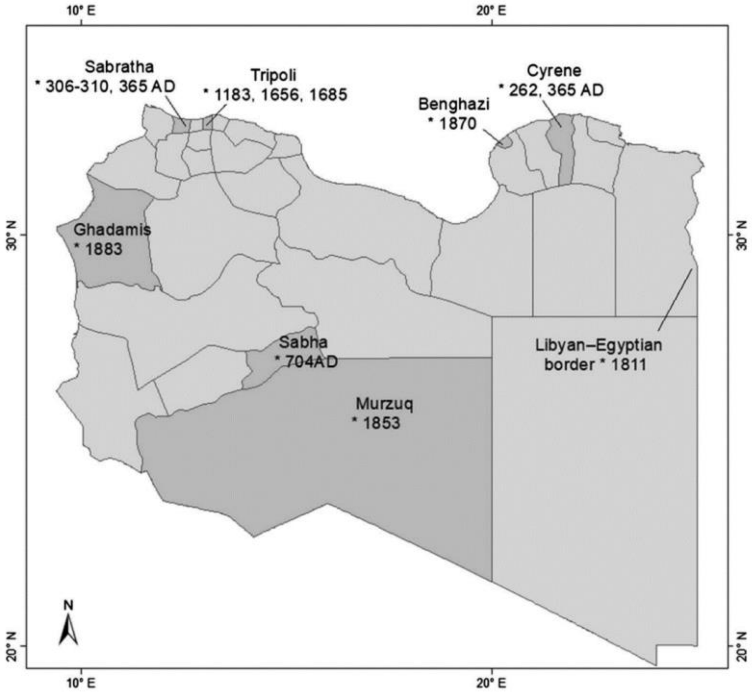

Figure 2.1 : map illustrates the seismic regions of Libya through the scope of time, from the era of Antiquity all the way to 1900 (Ambraseys, N.N. ,1984).

With the development of better seismographs, seismometers, and timing systems since the early 19th century, earthquake reports have increased. This has made seismology a more popular field and spurred further research. Reports on seismic activity in Libya appeared in various publications, though they weren't too specific about the exact locations. In Figures 2.3 and 2.4, all the available information from 1900-2019 is listed.

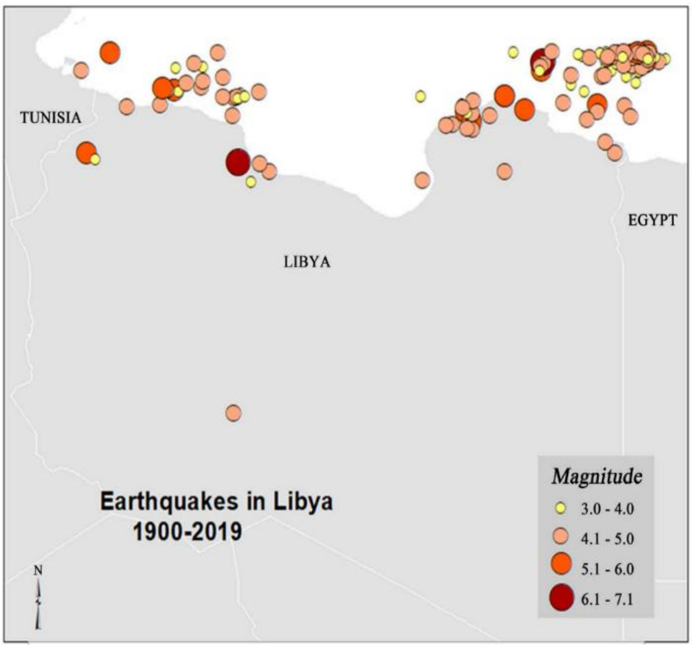

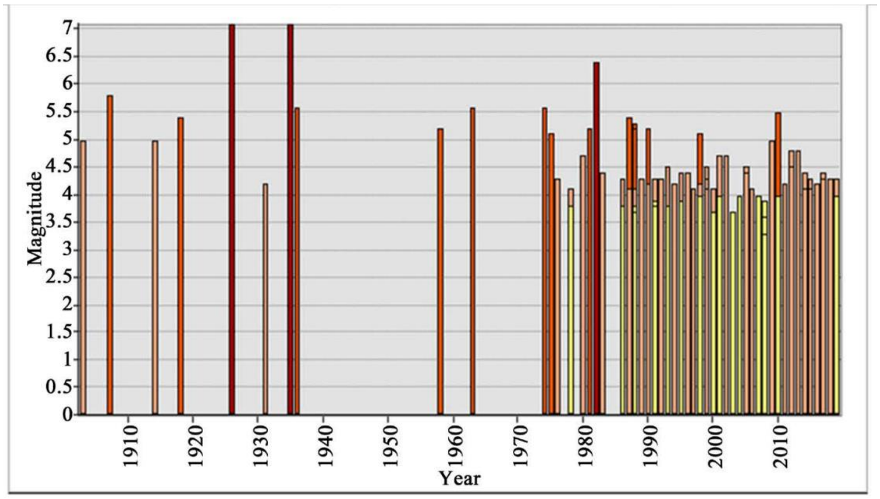

Figure 2.2 : This map illustrate the chronology and spatial distribution of earthquakes with a magnitude of 3.0 or greater that have occurred in or around Libya between 1900 and 2019. The affected area encompasses coordinates 20˚N - 34˚N and 10˚E - 25˚E, with color-coded events that differentiate them based on their occurrence over time (Ambraseys, N.N. ,1994).

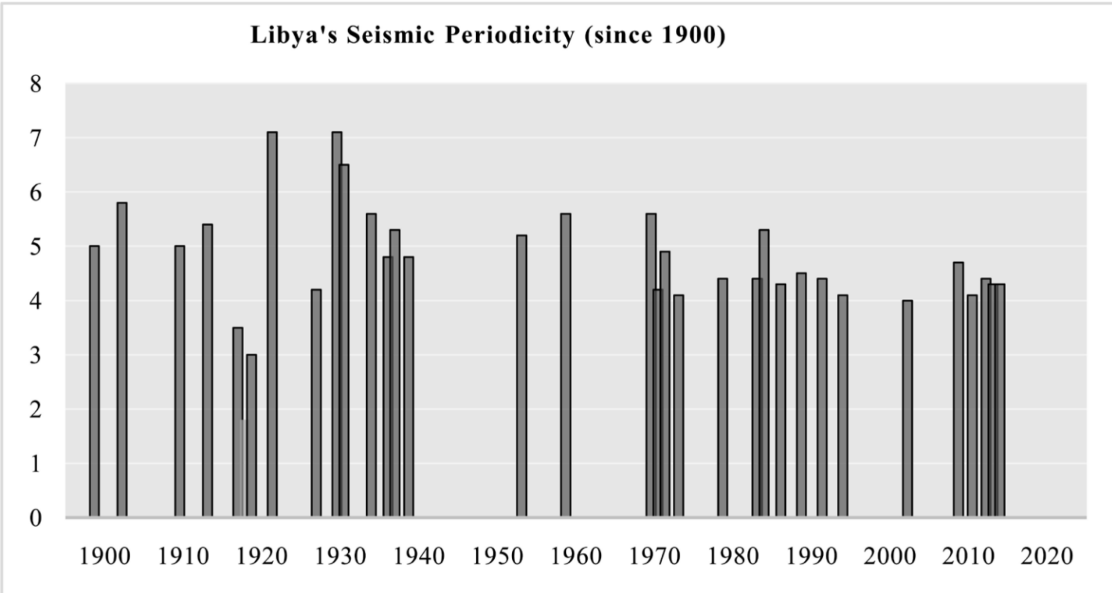

Figure 2.3 : Earthquakes affected Libya from 1903-2017 with magnitudes ranging from 4 - 8 (MR) (United States Geological Survey (USGS) , 2019).

The Eastern Hun Graben and its extension into the Mediterranean Sea mark the western side of the Gulf of Sirte where seismic activity is common in this region. There have been several earthquakes in this area. The tectonic movement has caused the land to slope upwards on the Libyan mainland and dip into the gulf. A series of earthquakes have been recorded in the northern coastal area of Libya between 1990 and 2019, as shown in Table 2.2.

Table 2.1: Earthquakes Striking Libya and Libyan coasts 1900-2019 (M ≥ 4.0).

Date A. D. Year m: d:	Time G. M. T. H: m: s:	Location Lat ˚N Long ˚E	Magnitude (Descriptive or Richter)	Location and Remarks
1903 11 22	----	32.80 13.20	5.0	Tripoli
1907 2 2	09:04:00	33.0 21.00	5.8	Offshore in North Cyrenaica
1914 5 18	10:46:00	31.30 22.00	5.0	A violent earthquake demolished the Gheddahia blockhouse
1918 10 14	14:06:00	33.0 22.0	5.4	Offshore: 10 km N of Susa
1919 8 3	----	31.5 19.5	----	Offshore: East Gulf of Sirte
1926 6 26	----	Hellenic arc	Small	Cyrenaica and Tripoli
1926 8 30	12:40:00	Hellenic arc	7.1	Benghazi and Derna
1931 4 24	15:21:00	32.1 19.9	4.2	Offshore: East Gulf of Sirte
1935 4 19	15:23:22	31.5 15.2	7.1	In area of Hun Graben
1935 4 20	05:10:51	31.0 15.5	6.5	8 tremors recorded in this area in the period April 19-29, 1935
1936 6 13	00:32:39	32.7 22.5	5.3 - 5.9	15 km West of Derna
1939 1 23	02:22:46	31.5 16.0	5.6	Gheddahia, aftershocks in cities along Libyan Coast
1940 1 2	----	30.3 22.0	4.8	South of Jabal al Akhdar area
1941 3 4	23:45:00	30.7 15.7	5.3-5.9	Hun Graben area
1941 5 3	23:45:10	33.3 23.5	----	Offshore: 100 km NE of Derna
1943 7 16	01:54:00	33.0 21.5	4.8	Offshore: ~45 km WNW of Susa
1948 5 22	----	33.3 23.5	----	Offshore: 100 km NE of Derna
1957 5 2	02:00:00	----	Minor	Felt in Northern Cyrenaica

1958 5 17	05:25:33	31.8 11.3	5.2	Jabal Nefusa area, E. Nalut
1963 2 21	17:14:31	32.6 20.9	5.6	Barce (Al-Marj) badly damaged
1974 9 4	06:29:16	33.05 13.5	5.6	Tripoli
1975 01 01	07:03:51	32.4 21.2	4.2	Al-Marj
1976 12 19	21:21:53	33.01 13.97	4.9	Tripoli
1978 6 7	07:21:21	25.7 15.0	4.1	North of Murzuq
1983 10 17	22:39:07	31.2 15.9	4.4	North of Sirte
1988 01 28	19:12:17	32.2 21.1	4.4	Al-Marj
1988 01 28	05:48:08	32.4 21.1	5.3	Al-Marj
1990 05 18	18:27:51	31.7 24.7	4.3	North of Batnan
1993 09 9	00:32:40	32.3 20.6	4.5	Al-Marj
1996 10 30	10:43:02	32.3 20.5	4.4	North of Benghazi
1999 11 7	14:43:35	32.6 21.1	4.1	Al-Marj
2007 9 3	11:58:38	31.5 11.5	4.0	North of Nalut
2013 5 11	04:42:37	32.7 12.3	4.7	North of Zuwarah
2015 10 3	22:47:55	32.2 21.0	4.1	Al-Marj
2017 5 2	09:43:12	31.9 24.5	4.4	WNW of Bardiyah
2017 11 11	19:00:48	32.75 20.92	4.3	NNE of Al-Marj
2019 2 21	02:19:32	32.57 21.62	4.3	Bayda

Table 2.2 (continued) : Earthquakes Striking Libya and Libyan coasts 1900-2019 ($M \geq 4.0$).

Recent analysis of seismic activity from 1900-2019 has shown that most earthquakes are found in three areas: the Hun Graben, which runs through the Mediterranean and

Libya; Al Jabal Al Akhdar in northeast Libya; and the east-west axis from Tunisia to Al Aziziya and Houn. Most quakes along the Hun Graben occur on its eastern coast. Investigations from 1939-1972 show seismic activity spreads to the Mediterranean Sea. This fault zone, which caused earthquakes in 1935 and 1941, could be a potential hazard for the cities of Al-Khums, Zlitan, and Misratah (population 700,000), making up 10% of Libya's population in 2018. Additionally, tremors have been concentrated near Al-Marj, on the western side of Al-Jabal Al-Akhdar, with aftershocks occurring as recently as 2015. Also, there has been little volcanic activity in the eastern section of the Sirte Basin Rift System (Figure 2.5).

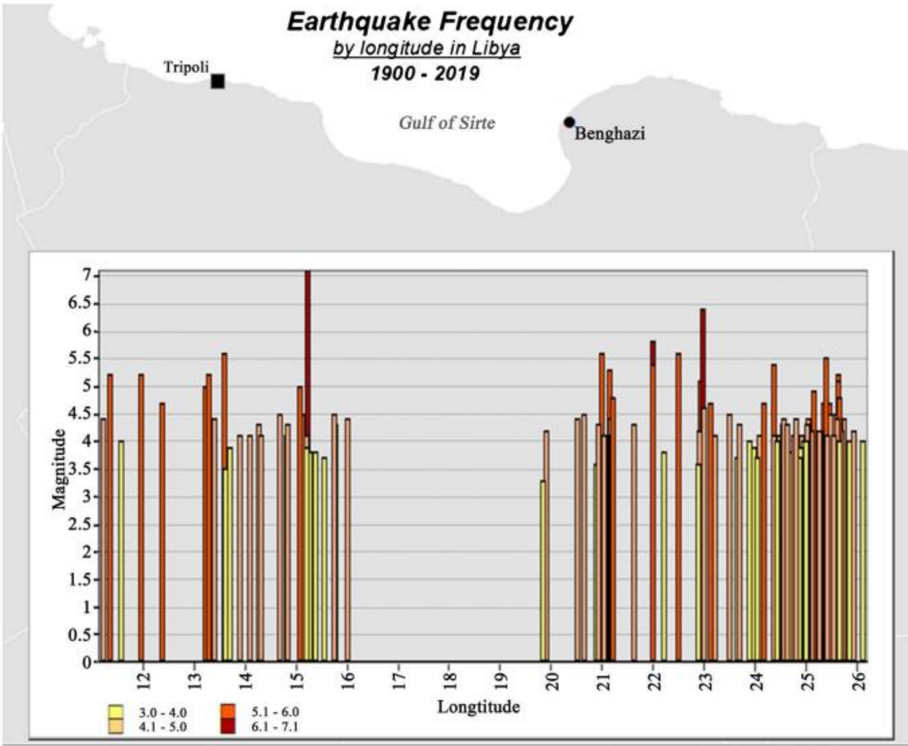

Figure 2.4 : Recent seismic mapping of Libya has revealed two distinct zones: West (III) and East (II). Plus, the area in the Gulf of Sirte in the middle seems to have experienced far fewer earthquakes since the turn of the century (Ambraseys, N.N. , 1994).

2.3 The 1963 Earthquake

In 1963, Al-Marj was destroyed, and then rebuilt 3 miles (5 km) from the original city. The new city is located 90 km (56 miles) northeast of Benghazi and is the administrative hub of the Marj District. Al-Marj and Darnah (figure 2.6) are the primary hubs for services and commerce, as well as key agricultural areas with a focus on fisheries, in Libya. It has been suggested that the escarpments seen are the consequence of uplifted fault plains; however, erosion has caused the fault-defined cliffs to become worn. This resulted in the formation of a curved and fractured escarpment face as well as a flat plain. According to Figure 2.6, the coastal area of northeastern Libya in the Al-Jabal Al-Akhdar region is still susceptible to earthquakes.

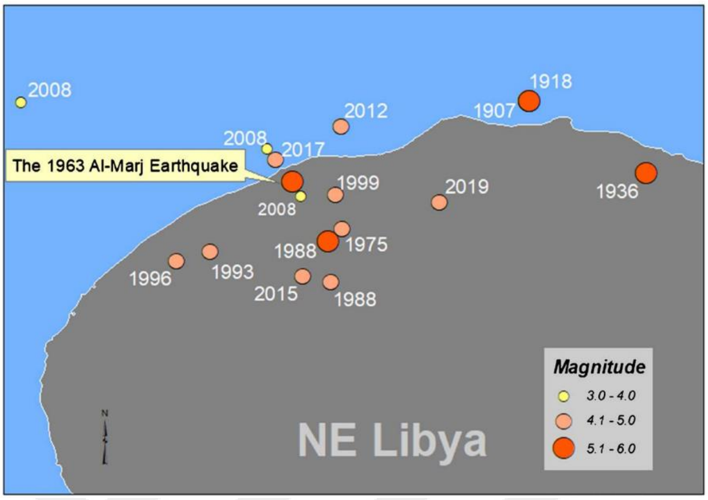

Figure 2.5 : The USGS has provided info on all the earthquakes that have happened around NE Libya in the last 119 years (1900-2019) (United States Geological Survey (USGS), 2018)

On 21 February 1963, at around 5:14 PM, an earthquake of magnitude 5.6 shook up the city of Al-Marj. The epicenter of the quake was 32.6˚N and 20.9˚E, with the focus of the tremor about 33 km down in the ground. The area suffered major damage, with most of the structures collapsing and the 13,000 people becoming homeless. 300 people lost their lives and 375 were injured. Five aftershocks with magnitudes higher than 4 came after the initial shock, continuing through the day (Table 2.3) (Gordon, D.W. and Engdahl, E.R. ,1963).

Table 2.3 : Basic data for the aftershocks (Gordon, D.W. and Engdahl, E.R. ,1963).

Date	Origin Time	Location Lat.(˚N) ong.(˚E)	Depth (km)	Magnitude	Stations Reporting
February 21	17:24:36	32.6˚ 21.1˚	33	4.0	7
February 21	18:33:00	32.9˚ 21.0˚	30	4.6	35
February 21	18:36:19	32.6˚ 21.0˚	30	4.0	9
February 21	20:26:40	32.6˚ 21.0˚	33	4.8-4.4	70
February 22	02:47:15	32.9˚ 21.1˚	33	4.3	23

As the city's buildings were made mostly of weak stone and clay, many people were injured, some died, and lots of property was damaged (Figure 2.7).

Figure 2.6 : Amid the ruins of a once thriving neighborhood lays a pile of rubble, with a collapsed roof made of wooden beams in the middle of it all. Even though the destruction is obvious, some structures, with sturdy frames and reinforced concrete columns, are still standing - though they've taken a beating from the force of nature (Minami, J.K., 1965).

The structure, composed of rubble stone encased in mud and/or clay, sustained extensive damage (Figure 2.8).

Figure 2.7 : An example of damage to a rubble stone and mud house (Sulfium Forum , 2010).

Houses made of sandstone or limestone, without any steel bars for reinforcement, were not able to resist the ground movement and created a danger to the inhabitants. The one-story dwellings created from hollow concrete blocks, though not reinforced, only had minor damage. On the other hand, it was only the structures with reinforced steel that were able to survive the disaster, and these were rare. As an example, the reinforced concrete elevated water tank and the adjacent five-story storage silo by the railway station were untouched by the disaster. (Figure 2.9).

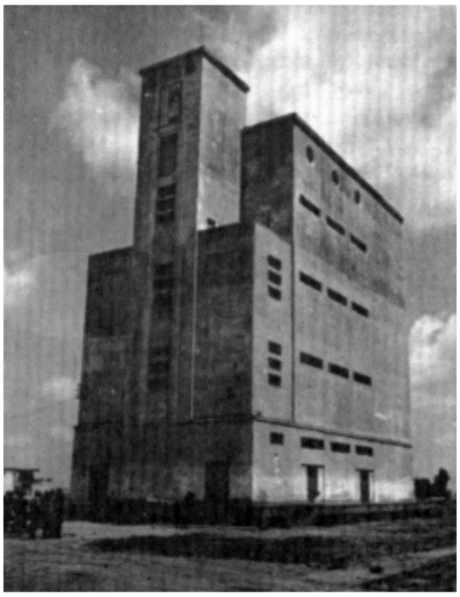

Figure 2.8: The five-storey silo building, constructed with reinforced concrete, was able to withstand the seismic forces (Minami, J.K., 1965).

3. MODERN ARCHITECTURE OF LIBYA

3.1 Introduction

Libya's architecture is a sign of a nation in perpetual change, seeking new and innovative ideas. People often assume that abandoning the past is a step forward, but this is not necessarily the case. Oil production has led to the construction of a variety of buildings - government offices, libraries, police stations, health centers, cultural clubs, schools, hotels, banks, etc. - that demonstrate the nation's political and social aspirations.

There has been much construction recently, however it often lacks personality. It would not take much to remedy this. However, effort needs to be put in to ensure Libya does not resemble any other modern nation's architecture. If the money devoted to architecture were put to use, it would be possible to create something unique. This would be something that takes into account the climate and geography of the area.

Rather than taking inspiration from magazine designs, designers should draw from the nation's heritage to create a specific kind of architecture, such as the Fezzan-Ghadames "Saharn Style" (Figure 3.1). Unfortunately, the past decade in Libya has seen a disconnect from Arab tradition and culture in regards to architecture and urban planning. Designers aim too often at forms and fetishes found in magazines, rather than being inspired by country dynamics.

Figure 3.1 : Saharn style - Fezzan-Ghadames (Tošković Dobrivoje,2006)

Traditional Libyan building still has elements applicable to buildings today. (Figure 3.2) takes a look at the transformation from traditional designs to more contemporary architecture, examining the progress, modifications, and the emergence of new housing, mosques, public spaces, businesses, health, and educational establishments.

Figure 3.2 : Traditional Libyan building (Tošković Dobrivoje,2006)

3.2 House Todays in Cities

The courtyard size has been reduced and is no longer relevant in domestic affairs, but it still offers some benefits. Nowadays, more space is used for private buildings on the streets. The courtyard is mainly for practical reasons, and the extra rooms are at the back, accessed via a hallway. Concrete walls or concrete blocks are usually constructed from concrete or travetti roofs. This is a rather plain design created by geometers with no consideration for the environment or local habitats. (Figure 3.3) shows what a courtyard looked like before the modern era.

Figure 3.3 : A house in Tripoli (Tošković Dobrivoje,2006)

3.3 The Villas

Villas have taken the place of old mansions in this country, usually with gardens and tall walls for privacy. The designs are usually based on those from the US and Western Europe. Instead of a central patio, there's a hallway that leads to the bedrooms and main rooms upstairs. Walls are made of stone, reinforced concrete, or concrete blocks. As for looks, three main styles are commonly seen - cosmopolitan, neo-classical, and a modern take on the classic Saharan style. Most villas aim for the cosmopolitan look, but it often looks copy-pasted and weird. Some still have a homey feel, like Libya (Figure 3.4).

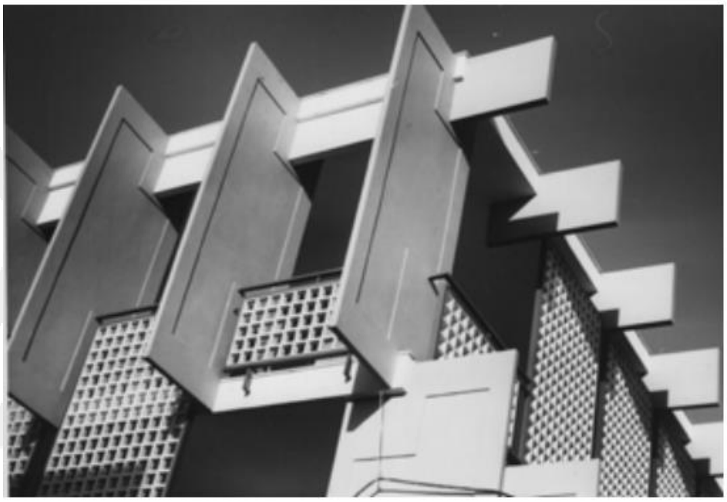

Figure 3.4 : A Villa in Libya (Tošković Dobrivoje,2006)

3.4 The Classical Style

This figure reveals the strong reaction people have to the unusual architecture of the Cosmopolitan Villa. It highlights two potential issues that architects should note: firstly, this design won't work in Libya's challenging climate and is not culturally or aesthetically linked to the country either, so replicating ancient styles is not the answer. Secondly, it's a setback to architectural knowledge advancement. Those who are stuck in an old school way of thinking can be just as much of an impediment to the creation of innovative domestic expression in architecture as those who lack romance or sentimentality in their designs. Most Libyans are not familiar with this type of building, and only the wealthy can afford it since it requires skilled artisans to decorate the walls. These artisans, like in other countries, are dwindling (Figure 3.5).

Figure 3.5 : Classical Style (Tošković Dobrivoje,2006)

3.5 The Modern Version of the Saharan Style

The Libyans are finally realizing that if they want to recreate the "wow-factor" of the Saharan Style, they need to look to their own culture for more ideas. Although some homes may have been designed to suit the climate, they lack the unique local touch. It is time to be mindful of the environment when living in a scorching sun and sand-blowing climate; incorporating local elements, being creative, and adding more shade and shadow can create a totally distinct style (Figure 3.6).

Figure 3.6 : The modren version of the "Saharan Style" (Tošković Dobrivoje,2006)

3.6 The Apartment Buildings

This new type of dwelling offers 120 square metres of living space for each family, with most having two to four stories. All of them have a loggia or balcony, along with a living room, two bedrooms, a dining room, a kitchen and a bathroom. These rooms can all be accessed via an entrance hall or corridor. In some dwellings there may even be two corridors, one for the main rooms and the other for the service areas or bathrooms. The framework is usually made of reinforced concrete, with some double-storey dwellings having concrete block bearing walls for infill walls instead. In some buildings, clay-mashrabiya is combined with a reinforced concrete framework to create a modern take on traditional verandahs (Figure 3.7).

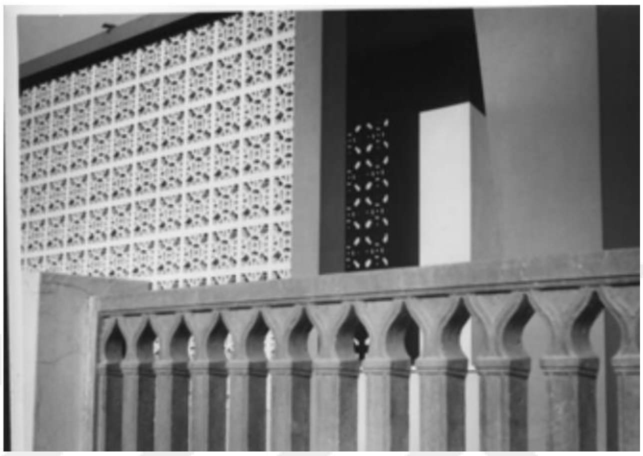

Figure 3.7 : The apartment buildings (Tošković Dobrivoje, 2006)

3.7 Multi Story Dwellings (Over Four Stories)

In Libya, there are hardly any eight-story buildings, mostly just a few in both Tripoli and Benghazi owned by private individuals and the government. The government is trying to make these buildings look modern and fancy, but it is making it difficult for Libyans to have any privacy in their homes as shown in Figure 3.8.

Figure 3.8 : Multi storey dwellings (Tošković Dobrivoje, 2006)

3.8 Administrative Buildings

Today's settlements are well-stocked with many public buildings recently built. The government has constructed plenty of offices around the country, ranging from basic Mudiriyah buildings to high-tech town halls to meet present and future needs. It is worth noting that buildings owned by businesses are usually of higher quality, as the owners can afford to invest in the architecture. They have chosen the designer carefully, taken their time with the design, and sought to make an impression and demonstrate their influence. Government buildings, on the other hand, are usually the result of state ambition (Figure 3.9) (Tošković Dobrivoje, 2006).

Figure 3.9 : Administrative buildings (Tošković Dobrivoje, 2006)

4. STRUCTURE DAMAGE ESTIMATION AND FRAGILITY CURVE

This section explains how to figure out how much damage different buildings might experience in an earthquake. Buildings are divided into four categories based on the seismic regulations they have to meet or don't have to meet: High-Code (HC), Moderate-Code (MC), Low-Code (LC) and Pre-Code (PC). Plus, there are Special High-Code (HS), Special Moderate-Code (MS), and Special Low-Code (LS) buildings which have been designed to more advanced design guidelines or retrofitted. Fragility curves and push-over curves are used to see how much damage the building might get depending on how much ground shaking there.

4.1 Input Requirements and Output Information

Building type, height, and seismic design level need to be known in order to estimate damage using fragility and capacity curves. Additionally, you must figure out the response spectrum, peak ground acceleration, and peak ground displacement for the building site. If you do not know the building type and seismic design level, the Hazus Inventory Technical Manual can help you make the connection between the seismic zone and occupancy. The probabilities of damage states are used to figure out physical destruction, economic, and social losses. Bear in mind that fragility and capacity curves are better for predicting average damage for larger groups, not individual buildings. To ensure accuracy, get an expert engineer to validate it (FEMA, 2020).

4.2 Form of Damage Functions

The Hazus Earthquake Building Damage Functions model fragility curves in the form of lognormal distributions. These curves show the likelihood of a building reaching or surpassing a certain damage state for a certain Peak Ground Motion (PGM) demand parameter, such as displacement from the response spectrum. Figure 4.1 depicts the damage states used in the generation of fragility curves. These curves are characterized by the median value of the PGM demand parameter (such as spectral displacement, spectral acceleration, Peak Ground Acceleration (PGA) or Peak Ground Displacement (PGD) that represents the threshold of the damage state, and by the variability related to that damage state. The spectral displacement, Sd, that marks the limit of a certain damage state is assumed to be distributed in the following equation 4.1.

$$S_d = \overline{S}_{d,ds} * \varepsilon_{ds} \tag{4.1}$$

Where

$\overline{S}_{d,ds}$ is the median value of spectral displacement of damage state, ds,

ε_{ds} is a lognormal random variable with unit median value and logarithmic standard deviation, β_{ds}

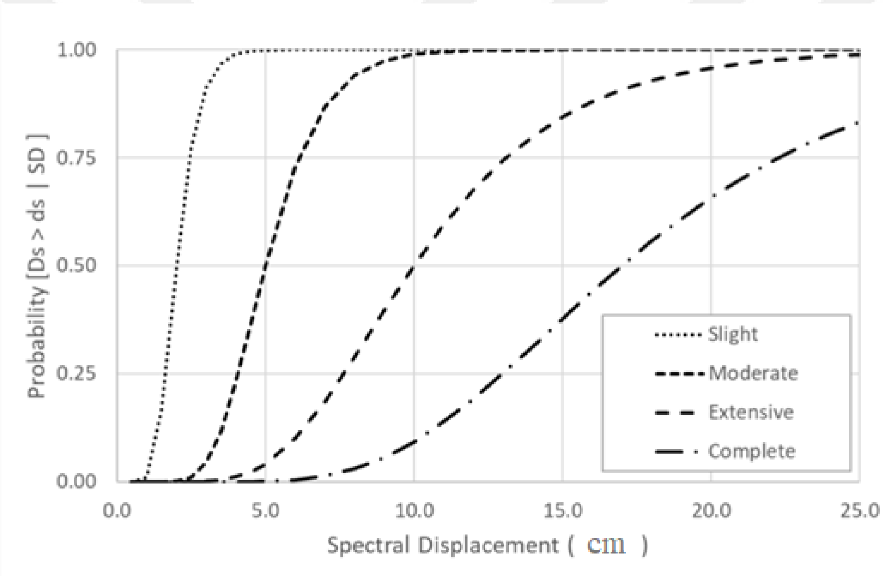

Figure 4.1 : Example Fragility Curves for Slight, Moderate, Extensive, and Complete Damage States (FEMA, 2020)

The log-normal standard deviation is basically the amount of randomness and uncertainty that contributes to the total variance. Kennedy et al. suggested that it is difficult to distinguish between randomness and uncertainty, so a combination of the two is used to create a "best-estimate" fragility curve. This curve is used to calculate the probability of a given damage state or surpassing it, taking into account the spectral displacement or other PEH parameters according to equation 4.2.

$$P[d_s|S_d] = \Phi\left[\frac{1}{\beta_{ds}}\ln\left(\frac{S_d}{\overline{S}_{d,ds}}\right)\right] \tag{4.2}$$

Where:

$\overline{S}_{d,ds}$ is the median value of spectral displacement at which the building reaches the threshold of the damage state, ds

β_{ds} is the standard deviation of the natural logarithm of spectral displacement for damage state, ds, and

Φ is the standard normal cumulative distribution function.

The median spectral displacement (or acceleration) values and the total variability are determined by combining field measurements, experiments, and theoretical simulations for each distinct building type and damage stage that needs to be considered. By combining performance data from structural components, seismic experience data collected from past earthquakes, laboratory testing, analytical methods, expert opinion, and judgement, engineers are able to determine more effective building designs due to the variability of each damage state attributed to the multiple sources that make up the whole. This includes uncertainty in the damage state threshold, a wide range of variability in the capacity (response) characteristics of the particular type of building being studied, and the requirement for a more sophisticated approach due to the unpredictable levels of ground motion (Hazus, 2020).

It has been hypothesized that the three primary elements leading to the variability of damage are lognormally distributed random variables. Fragility curves are derived from a PEH parameter, which, in the case of ground failure, is PGD, as opposed to the peak spectral response in displacement or acceleration when assessing damage from ground shaking. PGA (Peak Ground Acceleration) is taken into account when evaluating damage to structures such as those in the utility and transportation networks due to seismic activity. The highest point of spectral displacement is identified by understanding the characteristics of the building's reaction. To demonstrate the displacement of a certain structure and its seismic design level when exposed to a lateral earthquake load, the capacity spectrum approach is used. This method is similar to the one outlined by Mahaney et al. (1993) and outlined by FEMA (1996a) in their NEHRP Guidelines for the Seismic Rehabilitation of Buildings, and further detailed in the Seismic Evaluation and Retrofit of Concrete Buildings (SSC, 1996) as one of the two nonlinear static analysis methods (FEMA Hazus, 2020).

The PEH input spectrum serves as the foundation for the demand spectrum, which takes into account the utilization of better damping methods such as elastic damping and post-yield hysteretic damping linked to the cyclical reaction of the structure. As illustrated in Figure 4.2, the intersection between a standard building capacity curve and a standard demand spectrum (with an effective damping of more than 5% of critical) is visible. It is of the utmost importance to consider the design, yield, and ultimate capacity points when forming the building capacity curve. The peak building response (spectral displacement or spectral acceleration) at the intersection of the capacity curve and the demand spectrum is then used, along with fragility curves, to assess the likelihood of damage states (Hazus, 2020).

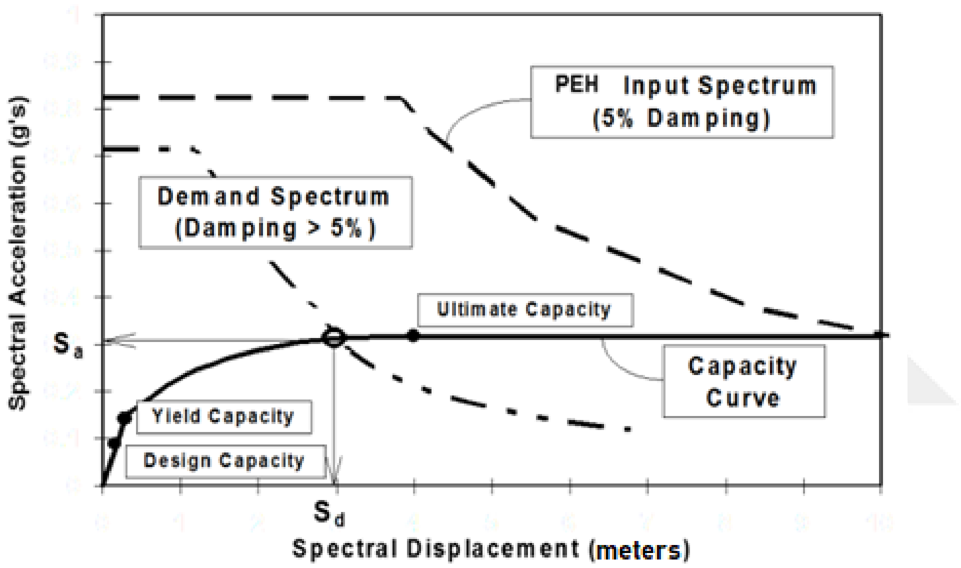

Figure 4.2 : Example building capacity curve and demand spectrum (Hazus, 2020)

4.3 Description of Specific Building Types

The Hazus Methodology provides a comprehensive breakdown of the 36 building types that are based on the FEMA 178 classification system. This system is outlined in the National Earthquake Hazards Reduction Program (NEHRP) Handbook for the Seismic Evaluation of Existing Buildings (FEMA, 1992). Furthermore, this methodology further divides these FEMA 178 classes into various height categories and includes mobile homes. Table 4.1 provides a detailed illustration of this breakdown (Hazus, 2020).

Table 4.1: Specific building types (FEMA, 2020)

#	Label	Description	Height			
			Range		Typical	
			Name	Stories	Stories	Meters
1	W1	"Wood, Light Frame (≤ 464.5 sq. m.)"		1 - 2	1	4
2	W2	"Wood, Commercial & Industrial (> 464.5 sq. m.)"		All	2	7
3	S1L	"Steel Moment Frame"	Low-Rise	1 - 3	2	7
4	S1M		Mid-Rise	4 - 7	5	18
5	S1H		High-Rise	8+	13	50
6	S2L	"Steel Braced Frame"	Low-Rise	1 - 3	2	7
7	S2M		Mid-Rise	4 - 7	5	18
8	S2H		High-Rise	8+	13	50
9	S3	"Steel Light Frame"		All	1	
10	S4L	"Steel Frame with Cast-in-Place Concrete Shear Walls"	Low-Rise	1 - 3	2	7
11	S4M		Mid-Rise	4 - 7	5	18
12	S4H		High-Rise	8+	13	50
13	S5L	"Steel Frame with Unreinforced Masonry Infill Walls"	Low-Rise	1 - 3	2	
14	S5M		Mid-Rise	4 - 7	5	
15	S5H		High-Rise	8+	13	
16	C1L	"Concrete Moment Frame"	Low-Rise	1 - 3	2	6
17	C1M		Mid-Rise	4 - 7	5	15
18	C1H		High-Rise	8+	12	36.5
19	C2L	"Concrete Shear Walls"	Low-Rise	1 - 3	2	6
20	C2M		Mid-Rise	4 - 7	5	15
21	C2H		High-Rise	8+	12	36.5
22	C3L	"Concrete Frame with Unreinforced Masonry Infill Walls"	Low-Rise	1 - 3	2	6
23	C3M		Mid-Rise	4 - 7	5	15
24	C3H		High-Rise	8+	12	36.5
25	PC1	"Precast Concrete Tilt-Up Walls"		All	1	4.5
26	PC2L	"Precast Concrete Frames with Concrete Shear Walls"	Low-Rise	1 - 3	2	6
27	PC2M		Mid-Rise	4 - 7	5	15
28	PC2H		High-Rise	8+	12	36.5
29	RM1L	"Reinforced Masonry Bearing Walls with Wood or Metal Deck Diaphragms"	Low-Rise	1 - 3	2	6
30	RM1M		Mid-Rise	4+	5	15
31	RM2L	"Reinforced Masonry Bearing Walls with Precast Concrete Diaphragms"	Low-Rise	1 - 3	2	6
32	RM2M		Mid-Rise	4 - 7	5	15
33	RM2H		High-Rise	8+	12	36.5
34	URML	"Unreinforced Masonry Bearing Walls"	Low-Rise	1 - 2	1	4.5
35	URMM		Mid-Rise	3+	3	10.5
36	MH	Mobile Homes		All	`1	3

4.4 Structural Systems

A full examination of the 16 structural systems applicable to different building types is presented in the sections below. To find drawings of these structures and additional information about these types of buildings, refer to FEMA 454, "Designing for Earthquakes: A Manual for Architects" (2006), which is available from the FEMA library (Hazus, 2020).

- Reinforced Concrete Moment Resisting Frames (C1):

  Reinforced concrete frame structures vary in design and come in a wide array of systems. Though some of the older frames may not have been designed correctly and could potentially crumble or collapse in the event of an earthquake, contemporary frames built in areas prone to seismic activity are designed to be more flexible and less likely to fail during a seismic episode. Steel moment frame buildings stand in contrast to this, as they do not have the same degree of flexibility.

4.5 Description of Building Damage States

The results of computing the magnitude of harm discussed in this section (i.e., the level of damage expected for certain types of buildings when exposed to a certain degree of shaking) are used in other parts of the process to determine estimated losses:

1. Fatalities and other casualties caused by structural damage.

2. Monetary losses due to the destruction of buildings (i.e., the cost of repairing damaged buildings and their contents).

3. Financial losses caused by the destruction and closure of buildings (e.g., losses resulting from business interruptions).

4. The social effects (e.g., lack of housing) can be assessed through the predictions of building damage. In addition, these predictions can be used to identify the locations and building types that are most likely to be affected in the event of certain hypothetical earthquakes.

In order to address the needs of its users, damage predictions must provide a clear understanding of physical destruction and its resulting impacts on life-safety, socio-economic, functional, and financial outcomes. The best way to evaluate the degree of destruction to a structure is to list out the individual parts (e.g., beams, columns, walls, ceilings, pipes, HVAC equipment, etc.) and describe the damage with terms such as "shear walls are cracked", "ceiling tiles have fallen", "diagonal bracing is buckled", and "wall panels are out", as well as words like "some" and "most" to demonstrate the level of damage. Non-structural components of a building can incur significant financial and practical losses, as well as minor to moderate injuries, whereas structural components can bring about extensive financial losses. Consequently, it is essential to account for the damage to structural and non-structural components separately. Damage to a building is a function of the building's deformation and can range from "none" to "complete" with wall cracks varying in size from "hairline cracks" that are nearly invisible to cracks that span several inches. As it is not possible to portray damage as a continuous function, the methodology relies on generalized "ranges" of damage to illustrate it. This technique enables experts to make predictions about the degree of structural and nonstructural damage that can be categorized into five categories : None, Slight, Moderate, Extensive, and Complete. An example of this is the designation of a Damage State based on the range from Slight to Moderate damage. Guidelines for the different Damage States are provided for all types of buildings to identify the visible damage of structural and nonstructural elements. By utilizing this physical damage estimation method, it is possible to determine the likelihood of a building belonging to one of the five Damage States (Hazus, 2020).

4.6 Structural Damage

This part provides a breakdown of the potential structural damage that can occur to a certain type of building. It is important to note that the "None" state is not included in this description. It is expected that when a building is in the Complete damage state, a portion of the floor area will collapse. Taking the material and construction of the building into consideration, as well as the effects of earthquakes, this collapse is likely. Additionally, it is possible that the structural damage may not be visible due to architectural finishes or fireproofing, so the nonstructural components can be used to estimate the damage severity. It is assumed that any cracks present are less than 3 mm (1/8 inch) wide; any cracks larger than this are referred to as "large" cracks (Hazus, 2020).

- Reinforced Concrete Moment Resisting Frames (C1)

• Slight Structural Damage: In certain beams and columns near joint regions or inside the joints, there is the presence of flexural or shear type hairline cracks.

• Moderate Structural Damage: It is evident that most beams and columns have developed hairline cracks, whilst some frame elements in ductile frames have reached their yield capacity, as shown by the presence of larger flexural cracks and concrete spalling. In the case of nonductile frames, greater shear cracks and spalling might be observed.

• Extensive Structural Damage: Certain frame elements have been subjected to their maximum load, as shown in ductile frames by large bending cracks, broken down concrete, and buckled primary reinforcement; nonductile frame elements may have experienced shear or bond breakdowns at reinforcement joints, snapped ties or buckled main reinforcement in columns leading to partial collapse.

• Complete Structural Damage: There is a probability that the structure will be destroyed or is in the process of being destroyed due to the brittle breaking of non-flexible frame components or the lack of frame dependability. It is estimated that anywhere from 5-13% of the total area of C1 structures with Total destruction will have been destroyed.

4.7 Building Damage Due to Ground Shaking

In this part, we look at the capacity and fragility curves used to determine the extent of damage to the general building stock. The building stock is composed of structures built to High-Code, Moderate-Code, Low-Code, or Pre-Code seismic standards. Section 6 has special building damage functions to calculate damage to hospitals and other essential facilities that are constructed to higher seismic standards than normal. The capacity curves and fragility curves for High-Code, Moderate-Code, Low-Code, and Pre-Code buildings come from the 1976 Uniform Building Code, 1985 NEHRP Provisions, or their more recent versions. Additionally, Table 4.2 has the design criteria for different seismic design zones(Hazus, 2020).

Table 4.2 : The design criteria for different seismic design zones (Hazus, 2020)

Seismic Design Level	Seismic Zone (Uniform Building Code)	Map Area (NEHRP Provisions)
High-Code	4	7
Moderate-Code	2B	5
Low-Code	1	3
Pre-Code	0	1

The capacity and fragility curves show buildings that meet the latest seismic code standards. To get the most accurate modelling of new constructions (e.g. Census tracts), you should use a building damage function that matches the seismic zone or map area of the governing rules. For constructions that do not meet these standards, it is suggested to use a reduced seismic design level. For instance, in high seismic activity places (e.g. California coast), constructions after 1973 should be modelled with High-Code damage functions, those built after 1940 with Moderate-Code damage functions, and those built before 1940 (before seismic codes were even established) with Pre-Code damage functions, though only if there is no other option. And if there is an older structure that was not designed to withstand earthquakes, regardless of where it is located in the US, it is advised to use Pre-Code damage functions (Hazus, 2020).

4.8 Capacity Curves

Design capacity is needed for a building to meet seismic regulations, such as the 1994 NEHRP Provisions. Wind is not included in design capacity, so tall buildings with low to moderate seismic activity might have more strength than the code requires. You can determine a building's lateral seismic force resistance by considering design redundancies, conservative code demands, and the strength of the building materials. The ultimate capacity of the building is when the whole system reaches a plastic state and is expected to deform beyond that without compromising stability. The stiffness of the building is based on its true period, which is usually longer than the code period due to various factors. The capacity curve of the building transitions from elastic to fully plastic from the yield point to the ultimate point, and remains plastic after the ultimate point - as shown in Figure 4.3 (Hazus, 2020).

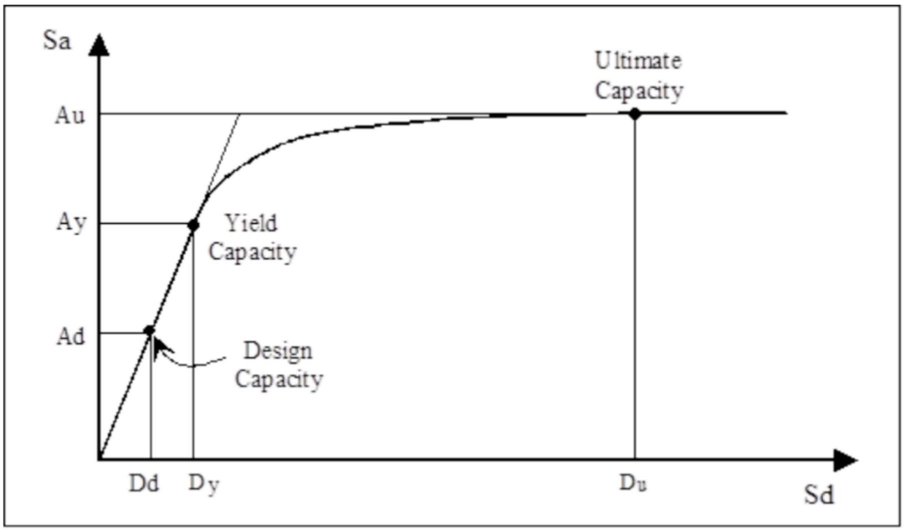

Figure 4.3 : Example building capacity curve (Hazus, 2020)

This building's capacity curves are determined using estimates of engineering features that are linked to the design, performance, and limits of each different type of building. These features are defined by the following aspects:

C_s design strength coefficient (fraction of building's weight),

T_e true "elastic" fundamental-mode period of building (seconds),

α_1 fraction of building weight effective in push-over mode,

α_2 fraction of building height at location of push-over mode displacement,

Γ "overstrength" factor relating "true" yield strength to design strength,

λ "overstrength" factor relating ultimate strength to yield strength,

μ "ductility" factor relating ultimate displacement to λ times the yield displacement (i.e., assumed point of significant yielding of the structure)

You can figure out the design strength, Cs, of a building by looking at the lateral-force design requirements in the most current seismic codes (like the 1994 NEHRP Provisions). These requirements depend on the seismic zone of the building's location, the soil condition of the site, and the building period, Te. Table 4.3 has design capacities for each type of lateral force-resisting system and building period, including

High-Code, Moderate-Code, Low-Code, and Pre-Code. It also has parameters for push-over mode and the ratio of ultimate yield strength. Table 4.4 and Table 4.5 show the values of the "ductility" factor for each building type and design level, respectively. Any building types shaded in the tables aren't allowed according to current seismic codes (Hazus, 2020).

Table 4.3: Code building capacity parameters - design strength (Cs) (Hazus, 2020)

Building Type	Seismic Design Level (Fraction of Building Weight)			
	High-Code	Moderate-Code	Low-Code	Pre-Code
C1L	0.133	0.067	0.033	0.033
C1M	0.133	0.067	0.033	0.033
C1H	0.067	0.033	0.017	0.017

Table 4.4: Code building capacity parameters - period (Te), pushover mode response factors and overstrength ratio (FEMA, 2020)

Building Type	Height to Roof (m)	Period, Te (Seconds)	Modal Factors		Overstrength Ratios	
			Weight,	Height,	Yield,	Ultimate,
C1L	6.0	0.40	0.80	0.75	1.50	3.00
C1M	15.0	0.75	0.80	0.75	1.25	3.00
C1H	36.5	1.45	0.75	0.60	1.10	3.00

Table 4.5: Code building capacity parameter – ductility (FEMA, 2020)

Building Type	Seismic Design Level			
	High-Code	Moderate-Code	Low-Code	Pre-Code
C1L	8.0	6.0	5.0	5.0
C1M	5.3	4.0	3.3	3.3
C1H	4.0	3.0	2.5	2.5

The capacity curves for structures have different characteristics depending on their ultimate strength. The figures in Tables 4.3, 4.4, and 4.5 are estimates of the median capacity. Buildings designed to the High-Code, Moderate-Code, and Low-Code seismic design levels have a variability of 0.25, while Pre-Code buildings have a variability of 0.30. Figure 4.4 shows the median, 84th percentile (+1), and 16th percentile (-1) capacity curves for an average building to demonstrate how variable the capacity curves are, as well as any other sources of variability and uncertainty, to calculate the total fragility curve (Hazus, 2020).

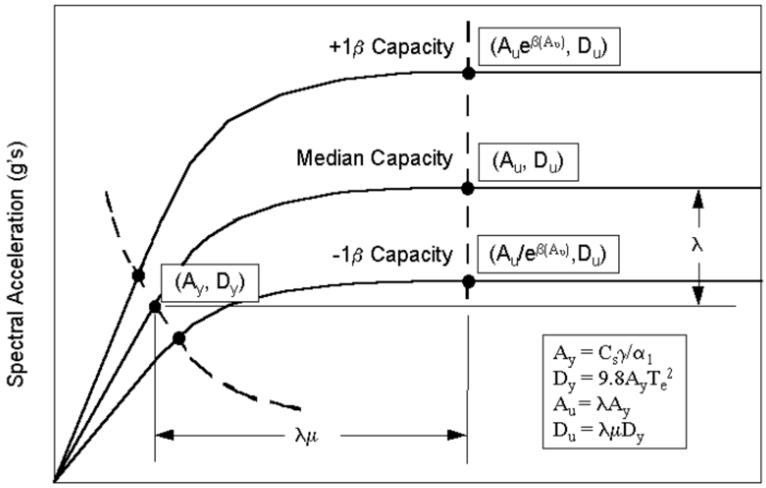

Figure 4.4 : Example construction of median, building capacity curves (Hazus, 2020)

Tables 4.6, 4.7, 4.8 and 4.9 give us a breakdown of the yield and ultimate capacity control points for each seismic design level: High-Code, Moderate-Code, Low-Code, or Pre-Code. Please note that the shaded boxes in each table do not comply with the current seismic codes, so they cannot be used.

Table 4.6 : Code Building Capacity Curves – High-Code Seismic Design Level (FEMA, 2020)

Building Type	Yield Capacity Point		Ultimate Capacity Point	
	Dy (m.)	Ay (g)	Du (m.)	Au (g)
C1L	0.391	0.250	9.387	0.749
C1M	1.152	0.208	18.436	0.624
C1H	1.152	0.098	24.13	0.293

Table 4.7 : Code building capacity curves – Moderate-code seismic design level (FEMA, 2020)

Building Type	Yield Capacity Point		Ultimate Capacity Point	
	Dy (m.)	Ay (g)	Du (m.)	Au (g)
C1L	0.196	0.125	3,52	0.375
C1M	0.576	0.104	6.914	0.321
C1H	1.005	0.049	9.049	0.147

Table 4.8 : Code building capacity curves – Low-code seismic design level (FEMA, 2020)

Building Type	Yield Capacity Point		Ultimate Capacity Point	
	Dy (m.)	Ay (g)	Du (m.)	Au (g)
C1L	0.098	0.062	1.467	0.187
C1M	0.288	0.052	2.881	0.156
C1H	0.503	0.024	3.77	0.073

Table 4.9 : Building Capacity Curves – Pre-Code Seismic Design Level (FEMA, 2020)

Building Type	Yield Capacity Point		Ultimate Capacity Point	
	Dy (m.)	Ay (g)	Du (m.)	Au (g)
C1L	0.098	0.062	1.467	0.187
C1M	0.288	0.052	2.881	0.156
C1H	0.503	0.024	3.77	0.073

4.9 Fragility Curve

4.9.1 Background

This piece goes over how to create fragility curves for various levels of structural and nonstructural damage - Slight, Moderate, Extensive, and Complete. These curves will tell us the median and lognormal standard deviation of the PEH demand. When it comes to structural damage, the PEH parameter used is spectral displacement, and for any nonstructural damage to acceleration-sensitive components, the PEH parameter used is spectral acceleration (FEMA Hazus, 2020).

4.9.2 Methodology

The likelihood of occupying or surpassing a predetermined level of damage can be represented in a lognormal cumulative distribution graph. In the context of structural damage, the probability of experiencing or having a higher degree of damage, given the spectrum displacement (Sd), can be expressed using equation 4.2.

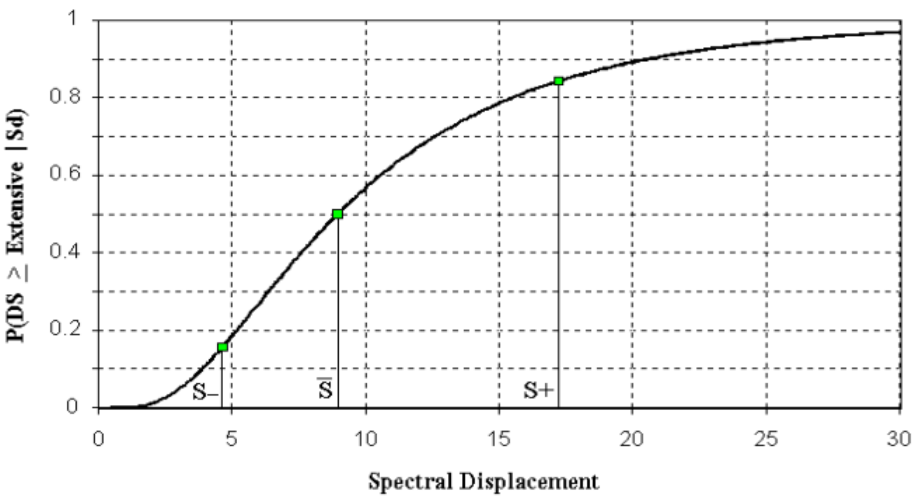

Figure 4.5 : Example Fragility Curve - Extensive Structural Damage, C1M Specific Building Type, High-Code Seismic Design (FEMA, 2020)

The fragility of structural components can be determined by analyzing the drift ratios that indicate the threshold of damage states. These damage state drift ratios can be transformed into spectral displacement by calculating them using Equation 4.3.

$$\overline{S}_{d,ds} = \delta_{R,S_{ds}} * \alpha_2 * h \quad (4.3)$$

Here

$\overline{S}_{d,ds}$	is the median value of spectral displacement, in centimeter, of structural components for damage state, d_s.
$\delta_{R,S_{ds}}$	is the drift ratio at the threshold of the structural damage state, d_s.
α_2	is the fraction of the building (roof) height at the location of push-pushover mode displacement.
h	is the typical roof height, in meters, of the specific building type of interest.

4.10 Structural Damage

The drift values for damage fragility curves are used to determine the amount of damage that different levels of shaking will cause to different types of buildings. These values may differ depending on the building and its seismic design level (Table 4.10) presents the drift ratios for low-rise buildings built to the latest seismic standards. Tables 4.11, 4.12, 4.13 amd 4.14 comprise a comprehensive list of drift ratios for all types and sizes of buildings, divided according to seismic design level (FEMA Hazus, 2020).

Table 4.4: Typical Drift Ratios Used to Define Median Values of Structural Damage (FEMA, 2020)

Seismic Design Level	Building Type (Low-Rise)	Drift Ratio at the Threshold of Structural Damage			
		Slight	Moderate	Extensive	Complete
High-code	C1L, S2L	0.005	0.010	0.030	0,080

Moderate-code	C1L, S2L	0.005	0.009	0.023	0.060
Low-Code	C1L, S2L	0.005	0.008	0.020	0.050
Pre-Code	C1L, S2L	0.004	0.006	0.016	0.040

Table 4.5 (continued) : Typical Drift Ratios Used to Define Median Values of Structural Damage (FEMA, 2020)

It is generally agreed that a moderate-code building which would totally collapse has a drift ratio of 75% of that of a high-code building, and for a low-code building it is 63%. Even though buildings with less ductile detailing have a lower post-yield capacity, the drift ratios for slight damage are the same for all building types, as the damage usually does not exceed the building's elastic capacity. To ensure that the ratio of slight to total destruction is the same as that of a high-code building, the drift ratios for moderate and extensive damage for moderate-code and low-code buildings are adjusted. Pre-code buildings use the drift ratios of low-code buildings, but these are lowered slightly to account for the lower performance expected from older buildings. This means that the drift ratio of a pre-code building is 80% of that of a similar low-code building.

Tables 4.11, 4.12, 4.13 and 4.14 show the median and lognormal standard deviation values for the different levels of structural damage - slight, moderate, extensive, and complete - for buildings rated high, moderate, low, and pre-code. The boxes that are shaded signify types that are not allowed by modern seismic codes (FEMA Hazus, 2020).

Table 4.6: Structural Fragility Curve Parameters - High-Code Seismic Design Level (FEMA, 2020)

Building Properties			Inter-Story Drift at Threshold of Damage State				Spectral Displacement (meters)							
Type	Height (meters)						Slight		Moderate		Extensive		Complete	
	Roof	Modal	Slight	Moderate	Extensive	Complete	Median	Beta	Median	Beta	Median	Beta	Median	Beta
C1L	6.0	4.5	0.0050	0.0100	0.0300	0.0800	0.90	0.81	1.80	0.84	5.40	0.86	14.40	0.80

Table 4.7: Structural Fragility Curve Parameters – Moderate Code Seismic Design Level (FEMA, 2020)

Building Properties			Inter-Story Drift at Threshold of Damage State				Spectral Displacement (meters)							
Type	Height (meters)						Slight		Moderate		Extensive		Complete	
	Roof	Modal	Slight	Moderate	Extensive	Complete	Median	Beta	Median	Beta	Median	Beta	Median	Beta
C1L	6.0	4.5	0.0050	0.0087	0.0233	0.0600	0.90	0.89	1.65	0.90	4.20	0.90	10.80	0.88

Table 4.8: Structural Fragility Curve Parameters - Low-Code Seismic Design level (FEMA, 2020)

Building Properties			Inter-Story Drift at Threshold of Damage State				Spectral Displacement (meters)							
Type	Height (meters)						Slight		Moderate		Extensive		Complete	
	Roof	Modal	Slight	Moderate	Extensive	Complete	Median	Beta	Median	Beta	Median	Beta	Median	Beta
C1L	6.0	4.5	0.0050	0.0080	0.0200	0.0500	0.90	0.95	1.44	0.91	3.60	0.85	9.00	0.97

Table 4.9: Structural Fragility Curve Parameters - Pre-Code Seismic Design Level (FEMA, 2020)

Building Properties			Inter-Story Drift at Threshold of Damage State				Spectral Displacement (meters)							
Type	Height (meters)						Slight		Moderate		Extensive		Complete	
	Roof	Modal	Slight	Moderate	Extensive	Complete	Median	Beta	Median	Beta	Median	Beta	Median	Beta
C1L	6.0	4.5	0.0040	0.0064	0.0160	0.0400	0.72	0.98	1.15	0.94	2.88	0.90	7.20	0.96

5.BUILDING DESCRIPTION (CASE STUDY)

5.1 Drawing of the Building

In this study, the most common types of a residential building in Libya are described in (Figure 5.1).

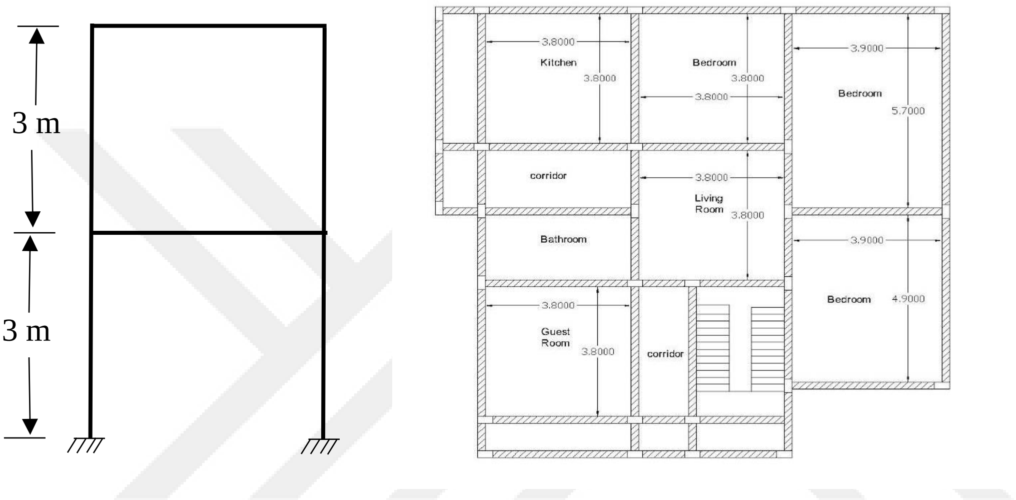

Figure 5.1: The Plan of The Residential Building of the Case Study

Two techniques have been used to construct residential houses, the first one is to use dropped beams with thin solid slabs and the second one is to use ribbed slabs with bands. Both systems are described in (Figures 5.2, 5.3, 5.4, 5.5).

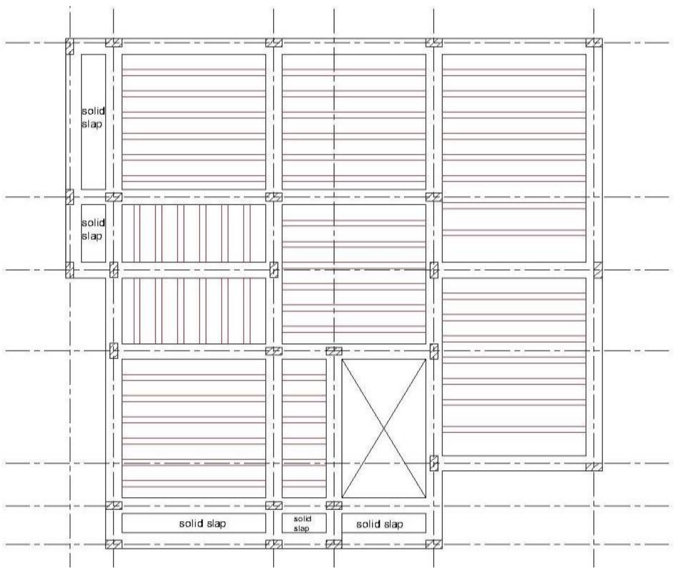

Figure 5.2: Type 1 of the Residentiel Building of the Case Study

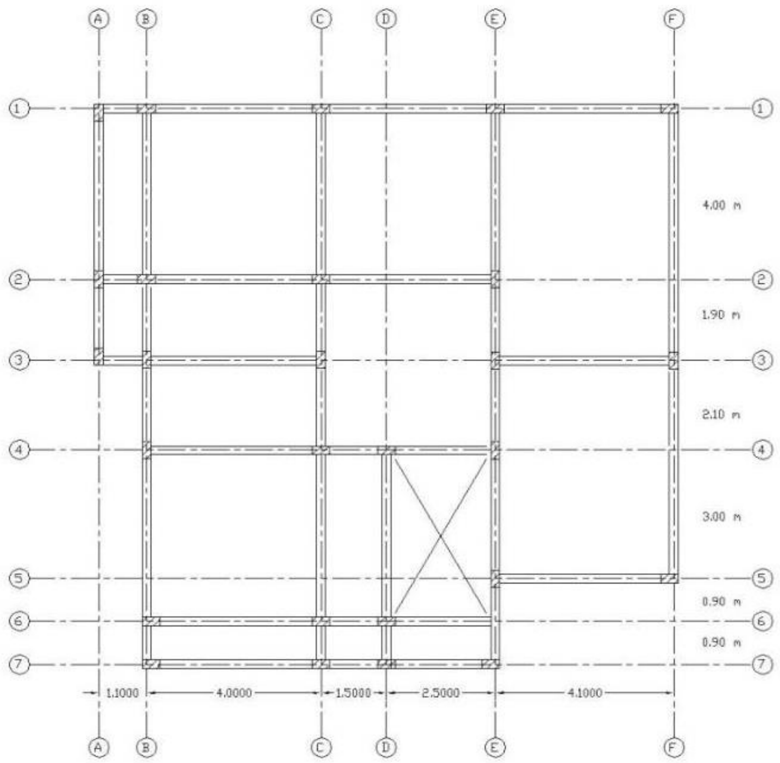

Figure 5.3: Type 2 of The Residential Building of The Case Study

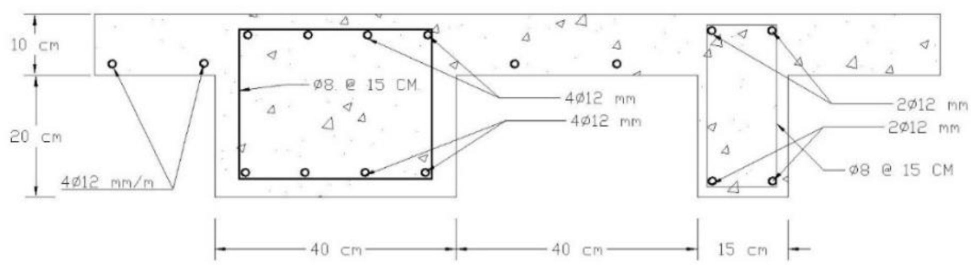

Figure 5.5: Band Beam and Sub-Beam Details for Type 2

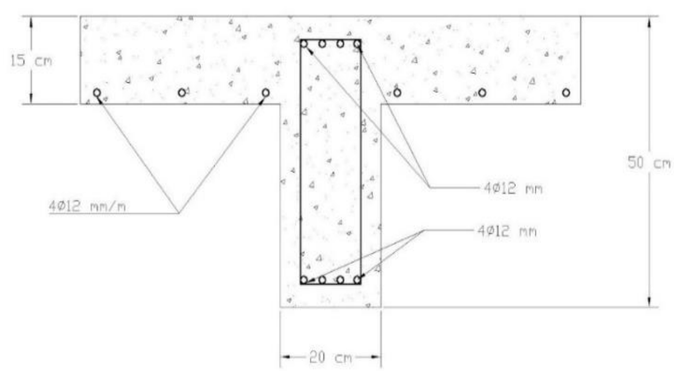

Figure 5.4: Dropped Beam Detail for Type 1

The detail of the column is shown in Figure 5.6.

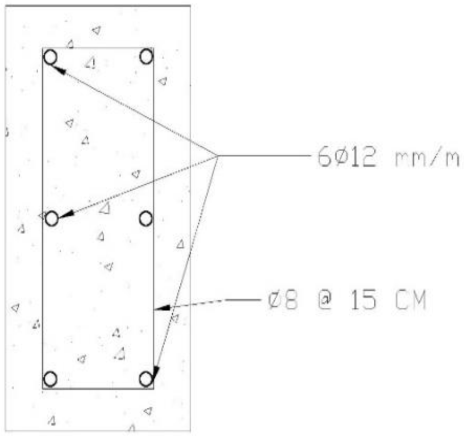

Figure 5.6: Typical Column Detail for Type 1&2

5.2 Material Properties

The properties of the materials used to construct residential houses are shown in Table 5.1.

Table 5.1: Material properties

Material	Properties
Concrete	f_c' =25 MPa
Steel	f_y =420 MPa

5.3 Load Distribution

The values of loads are shown in Table 5.2.

Table 5.2 : Types and values of applied loads

The Load	Type of loading	The value of the input
Self-Weight	All Members	Calculated By Program
Dead Load	Shell Area	3 KN/m2
Live Load	Shell Area	3 KN/m2

5.4 Modeling of The Buildings

The two study cases were modeled in SAP2000 Software as shown in Figure 5.7.

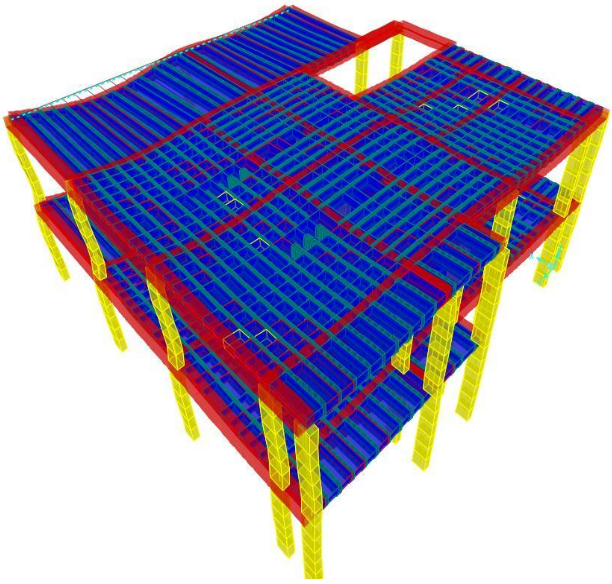

a- Type 1 Model in SAP2000

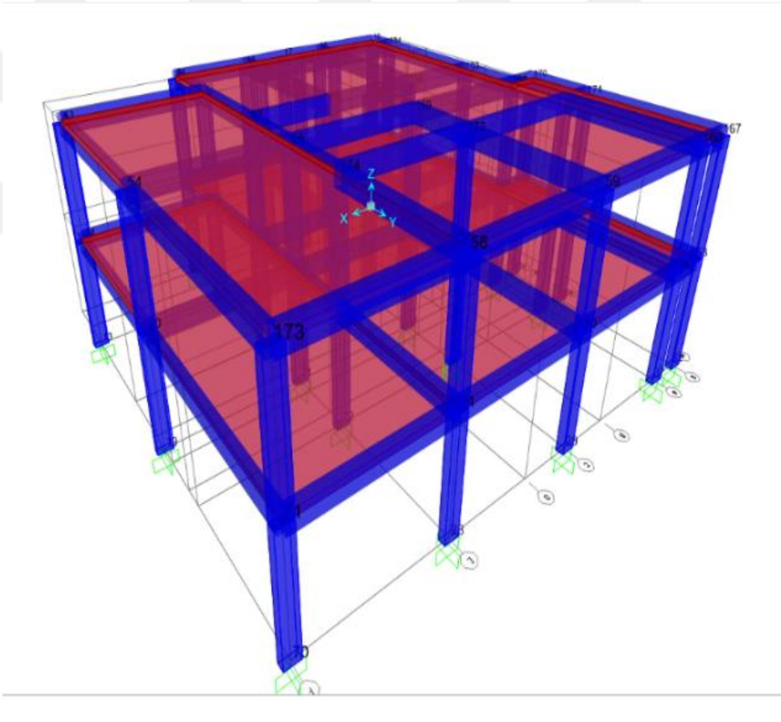

b- Type 2 Model in SAP2000

Figure 5.7: Type 1 and 2 models in SAP2000.

In the pushover analysis, the hinges are predicted at the potential weak areas and the sequence of damage at these hinge locations is tracked until the structure collapses. (Figure 5.8).

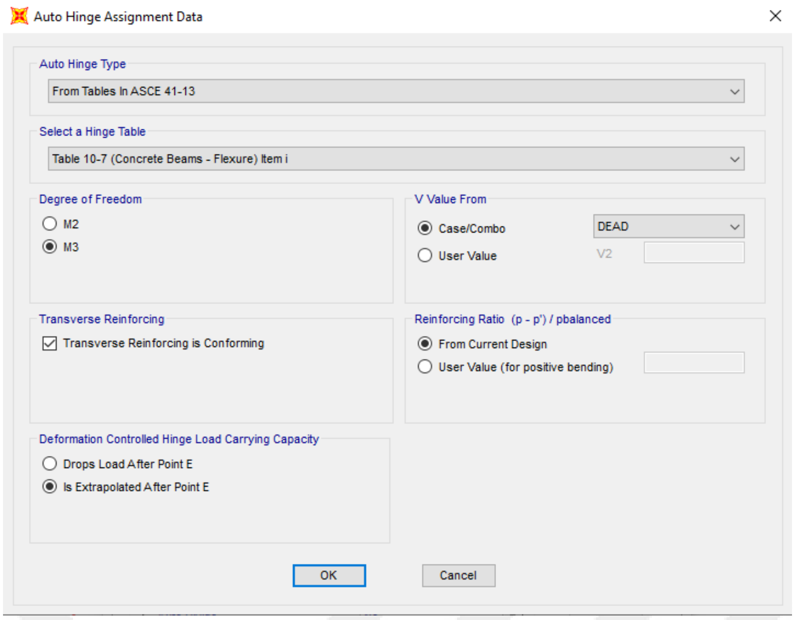

a

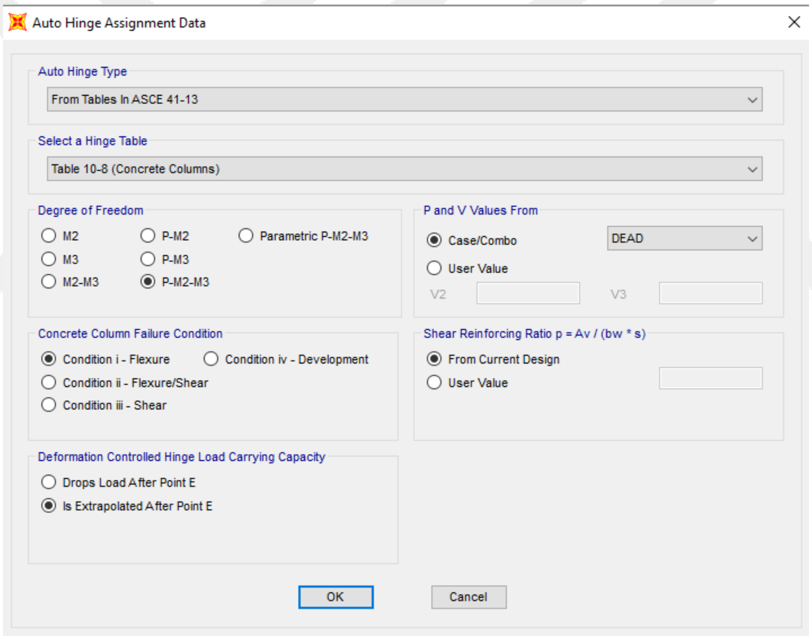

b

Figure 5.8: Hinges Assignments in SAP2000 for a-beams elements, b-columns elements.

5.5 Non-linear Static Push-over Analysis

The use of static pushover analysis to check the seismic performance of existing and new structures is becoming more widespread. It's expected that the pushover analysis will give adequate info about the seismic requirements imposed by the design ground motion on the structural system and its parts. This paper looks to summarize the ideas on which the pushover analysis is based, to assess the accuracy of the predictions, and to identify cases where the pushover results will be wrong or misleading. In recent years, there's been a need for more rigorous seismic design codes and a better understanding of engineering, making existing buildings seismically deficient. Earthquakes have shown that there's a need to evaluate and strengthen existing buildings, leading to the emergence of performance-based design and an increased need for non-linear static pushover analysis. This approach increases the load on the structure in stages, allowing weak links and failure modes to be identified. The ATC-40 and FEMA-273 documents are essential, as they provide the modeling and analysis procedures for pushover analysis, with different force-deformation criteria for different members. This article covers the steps taken to perform a pushover analysis of a three-dimensional building using SAP2000, a powerful three-dimensional structural analysis program.

The Push-Over in X and Y direction results are shown in (Figures 5.9 and 5.10).

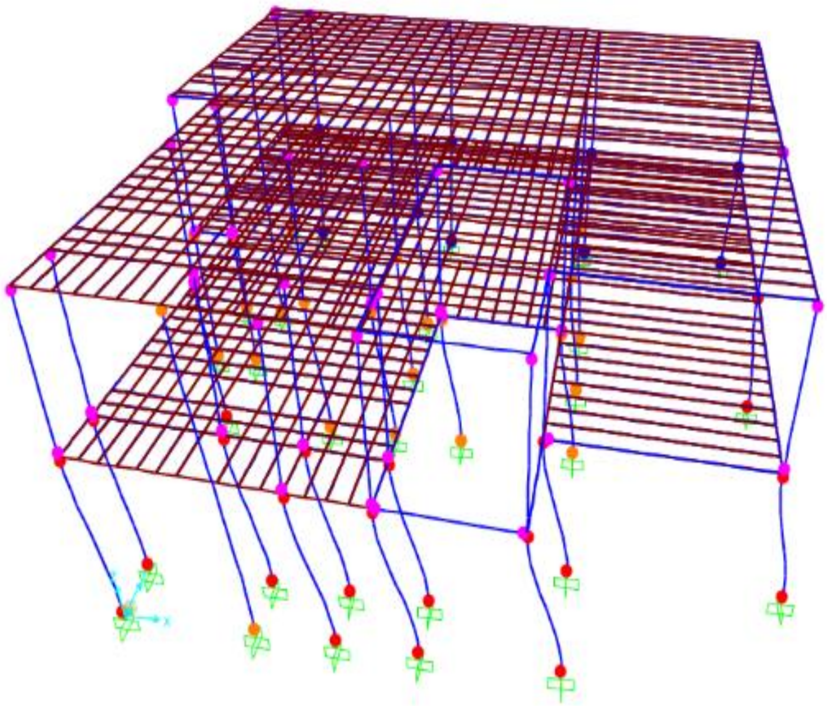

a- Push-Over in X Direction for Type 1

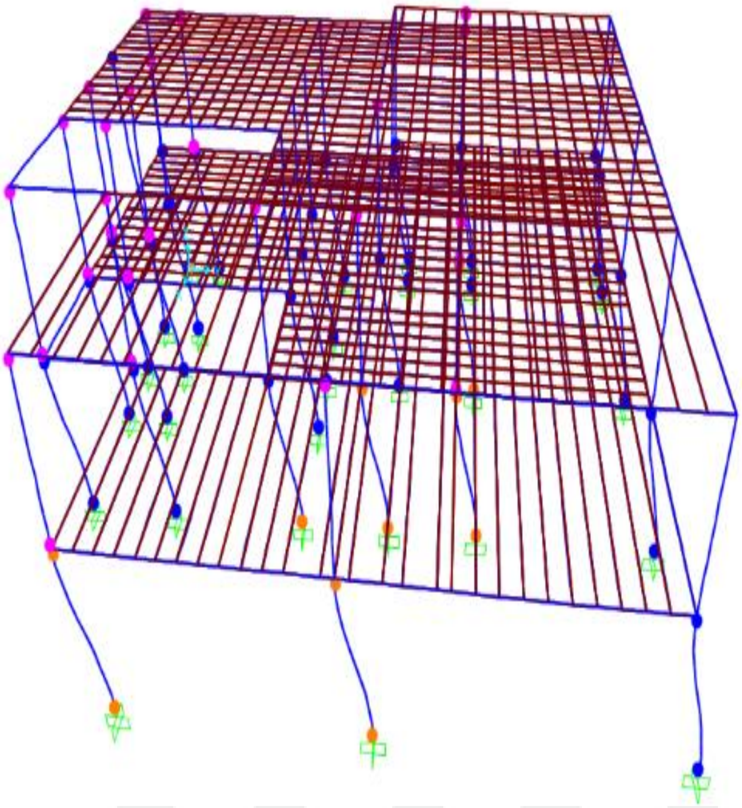

b- Push-Over in Y Direction for Type 1

Figure 5.9: Push-Over in X and Y direction for Type 1 in SAP2000.

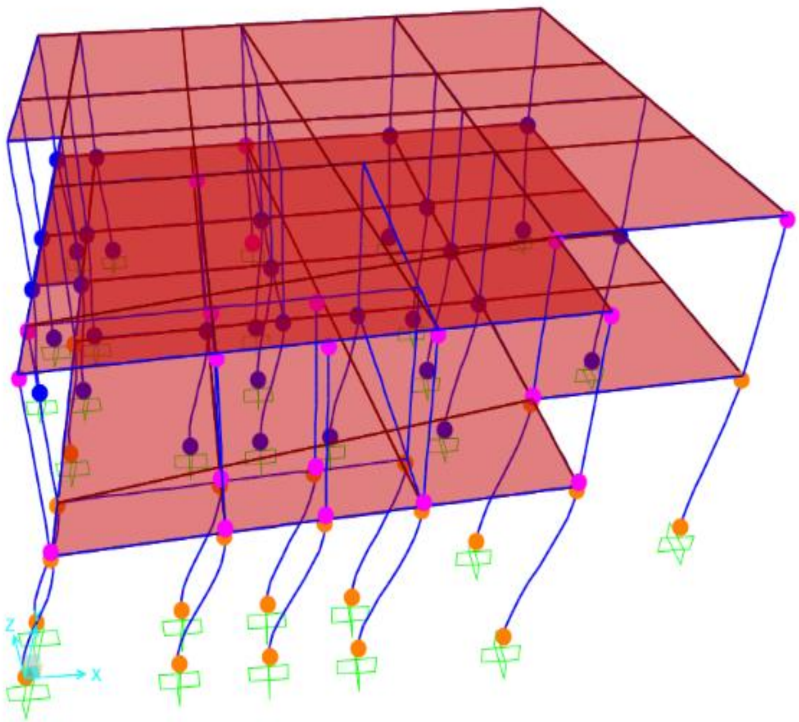

a- Push-Over in X Direction for Type 2

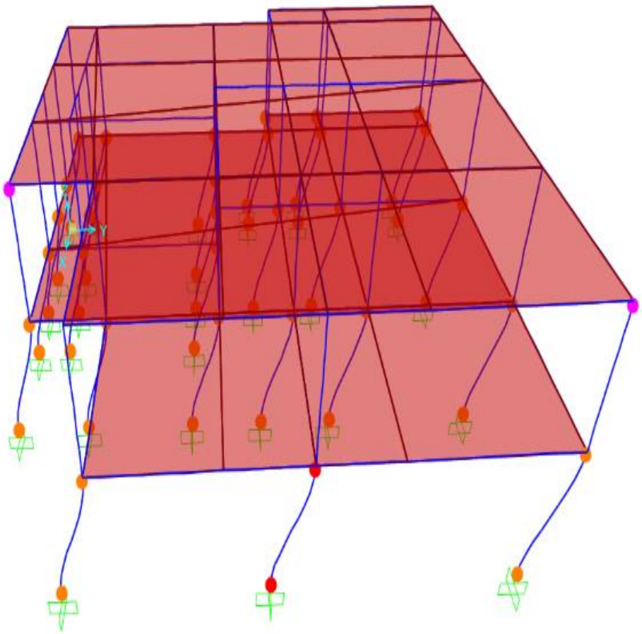

b- Push-Over in Y Direction for Type 2

Figure 5.10: Push-Over in X and Y direction for Type 2 in SAP2000.

5.6 Capacity Curves

A capacity curve (or push-over curve) is a chart that shows the relationship between the lateral load applied to a building and the lateral displacement that occurs. It is worked out by calculating the static-equivalent base shear and the amount the building (such as the roof) moves. The capacity curves in both the X and Y directions are displayed in the following figures (5.11, 5.12, 5.13, 5.14).

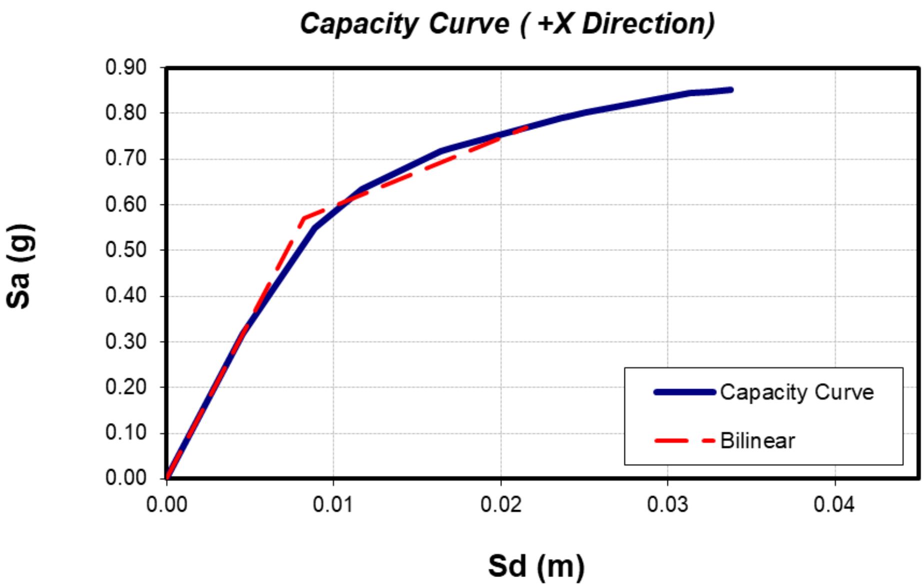

Figure 5.11 : Capacity Curve in X direction for Type 1 in SAP2000.

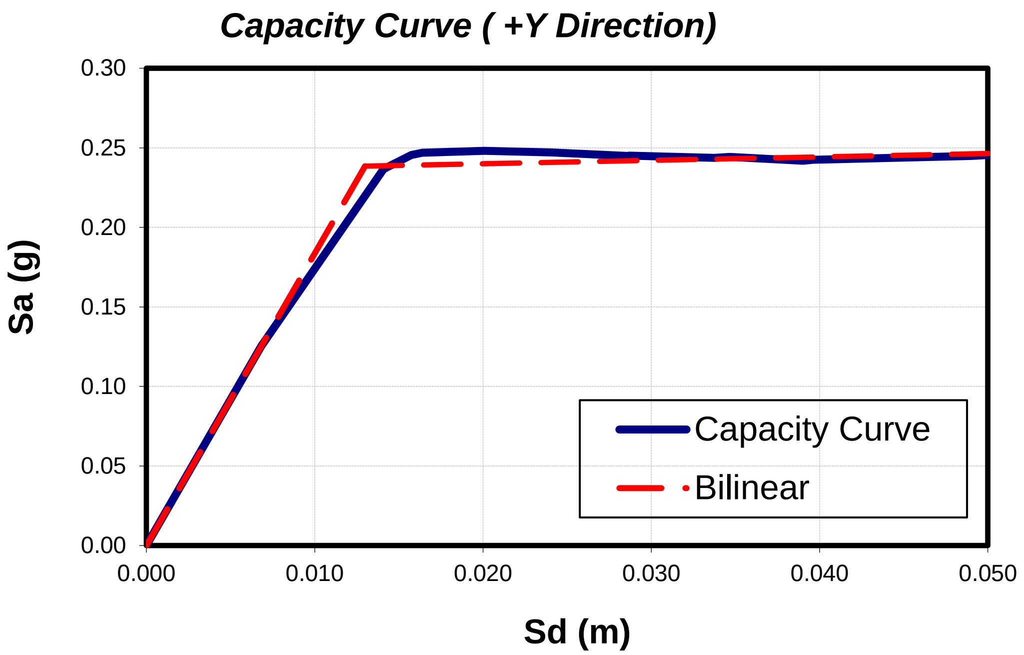

Figure 5.12 : Capacity Curve Y direction for Type 1 in SAP2000.

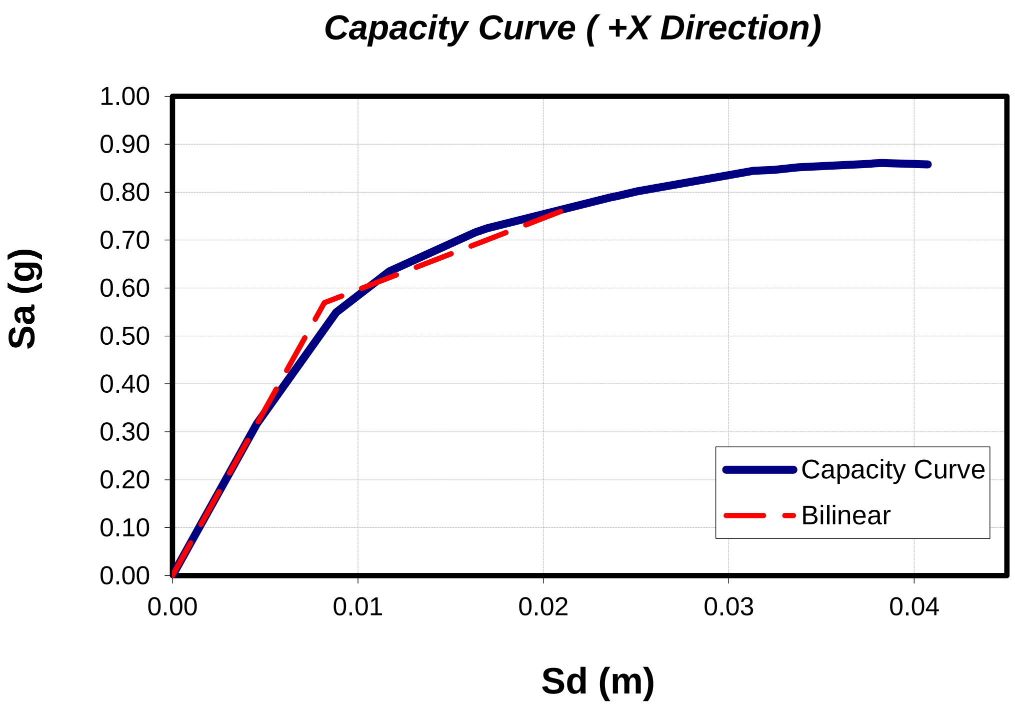

Figure 5.13 : Capacity Curve in X and Y direction for Type 2 in SAP2000

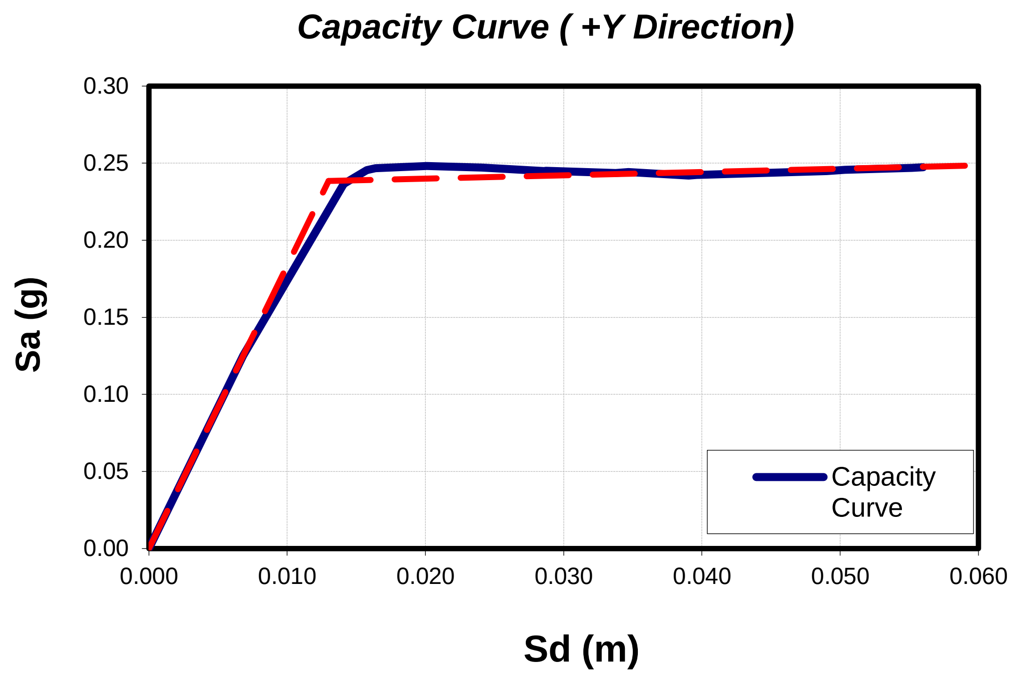

Figure 5.14 : Capacity Curve in X and Y direction for Type 2 in SAP2000

The results for type 1 are shown in (Table 5.3, 5.4, 5.5).

Table 5.3 : modal participation Ratio for type 1

Modal Participating Ratio			
Mode	Period	UX (%)	UY (%)
1	0.476333	0.10%	92.64%
2	0.248006	54.98%	0.18%

Table 5.4 : yield capacity for type 1

Yield Capacity			
	Dy (m)	Ay (m)	Du (m)
PushX	0.0097	0.6754	0.0216
PushY	0.0134	0.2459	0.0817
Average	0.0116	0.4606	0.0516
Min	0.0097	0.2459	0.0216

Table 5.5 : Damage States Thresholds for type 1

Damage States Thresholds (Mean Values) (cm)				
	Slight	Moderate	Extensive	Complete
PushX	2.292	4.259	9.817	22.800
PushY	1.662	2.878	6.603	15.897
Average	1.977	3.568	8.210	19.348

The results for type 2 are shown in Tables 5.6, 5.7 and 5.8.

Table 5.6 : Modal participation Ratio for type 2

Modal Participating Ratio			
Mode	Period	UX (%)	UY (%)
1	0.362171	0.064%	92.839%
2	0.18133	55.748%	0.156%

Table 5.7 : yield capacity for type 2

	Yield Capacity		
	Dy (m)	Ay (m)	Du (m)
PushX	0.0045	0.5846	0.0216
PushY	0.0075	0.2366	0.0817
Average	0.0060	0.4106	0.0516
Min	0.0045	0.2366	0.0216

Table 5.8 : Damage States Thresholds for type 2

Damage States Thresholds (Mean Values) (cm)				
	Slight	Moderate	Extensive	Complete
PushX	2.244	4.260	10.191	24.416
PushY	1.554	2.759	6.384	15.502
Average	1.899	3.510	8.288	19.959

The fragility curves for types 1 and 2 as shown in figure 5.15 and figure 5.16.

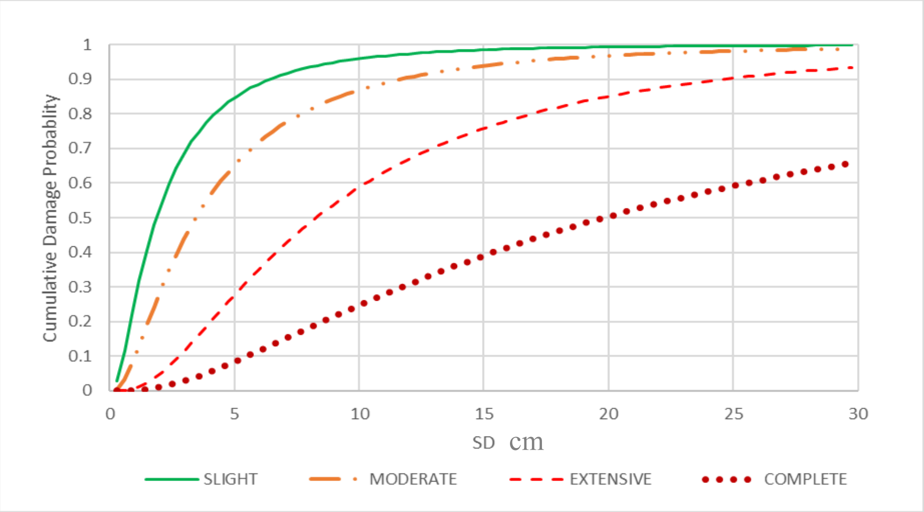

Figure 5.15 : Fragility Curve for Type1

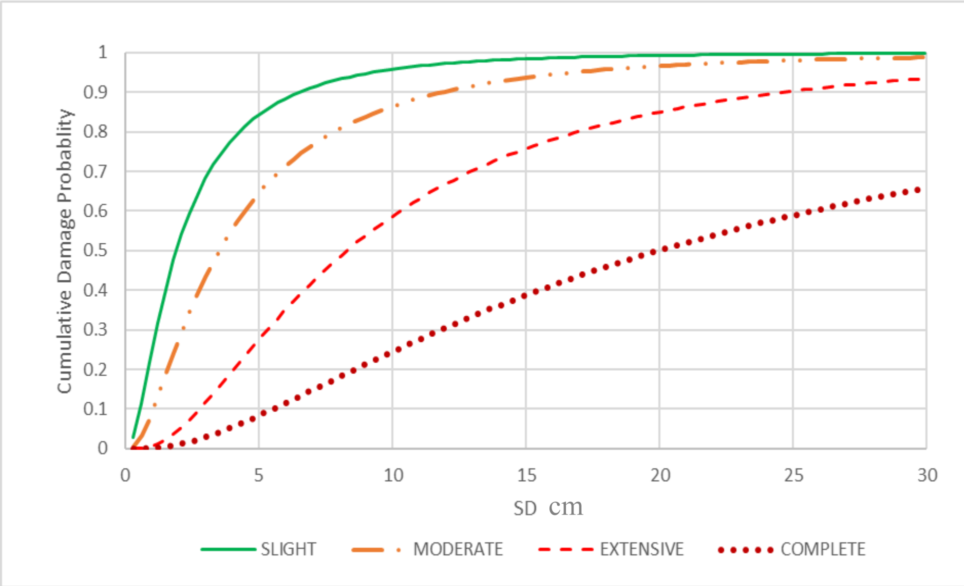

Figure 5.16 : Fragility Curve for Type 2

6. DISCUSSION

Generally, Libya is known to have a low seismic hazard. However, there is more activity in the area around Jabal al Akhdar Uplift and the Hellenic Arc Subduction Zone in the northeast. Surprisingly, the seismic hazard in northwest Libya comes from offshore events in the Misrata Basin, rather than the Hün Graben. Table 6.1 contains information for horizontal spectral acceleration with 5% damping for Peak Ground Acceleration (PGA), 0.2s (short period), 1.0s and 2.0s (long period) for return periods of 475 years and 2,475 years and for type C of soil (very dense soil and soft rock) (Table 6.1) (R. Lagesse, 2017).

Table 6.1: values of horizontal spectral acceleration for Misurata city s for a site with bedrock site conditions ($\boldsymbol{V_{s30}}$ ≥760m/s) (R. Lagesse, 2017)

Location	Period (s) and spectral acceleration (g)							
	PGA		0.2		1.0		2.0	
	475 year	2,475 year	475 year	2,475 year	475 year	2,475 year	475 year	2,475 year
Misurata	0.06	0.14	0.13	0.30	0.02	0.06	0.01	0.03

Figure 6.1, 6.2 are the spectral acceleration for Misurata city for different return years.

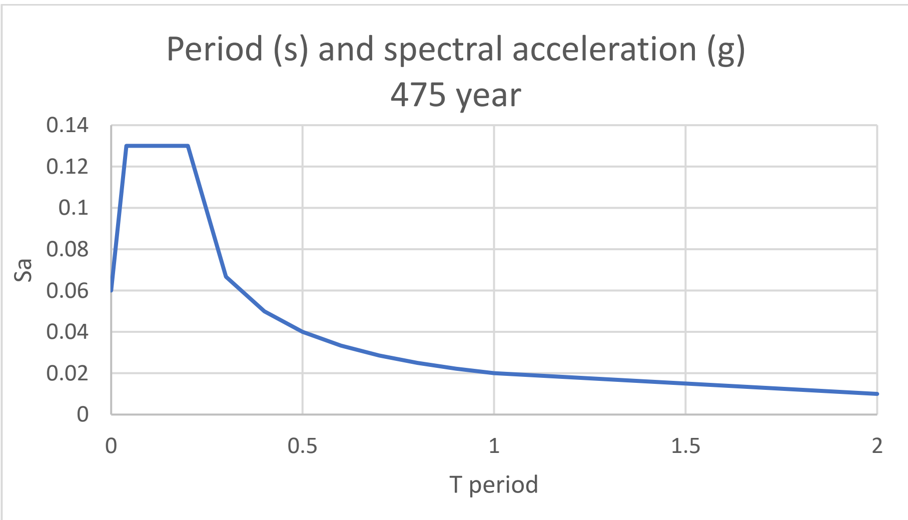

Figure 6.1 : Spectral acceleriation Misurata City for C type of soil and 475 year return

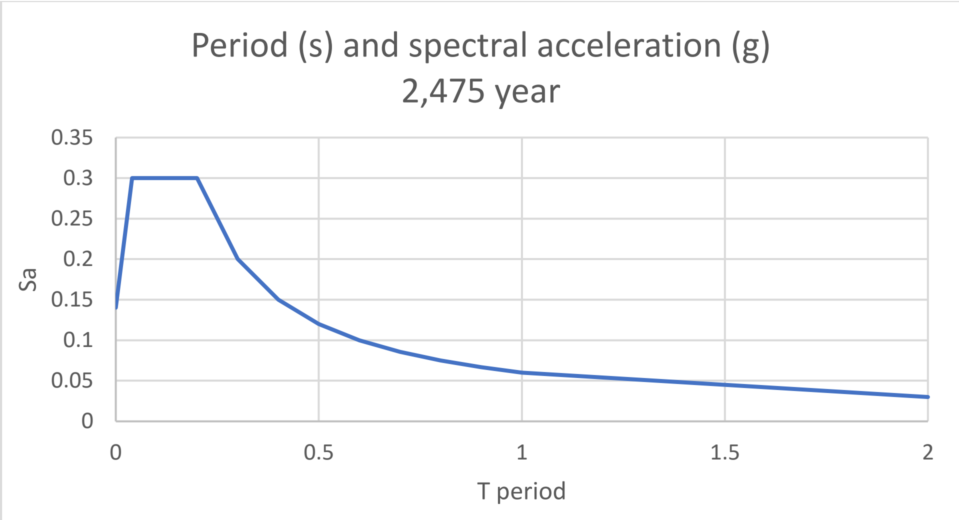

Figure 6.2 : Spectral acceleriation Misurata City for C type of soil and 2475 year return

The maximum target displacement for the two types using push-over curves in both x and y directions are shown in figures 6.3, 6.4.

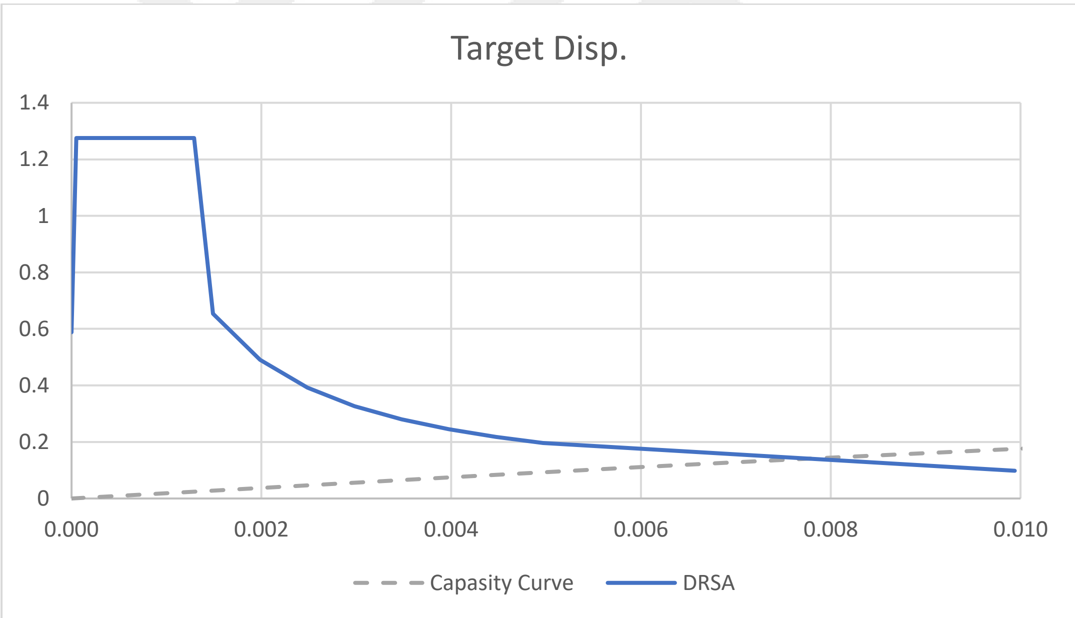

a

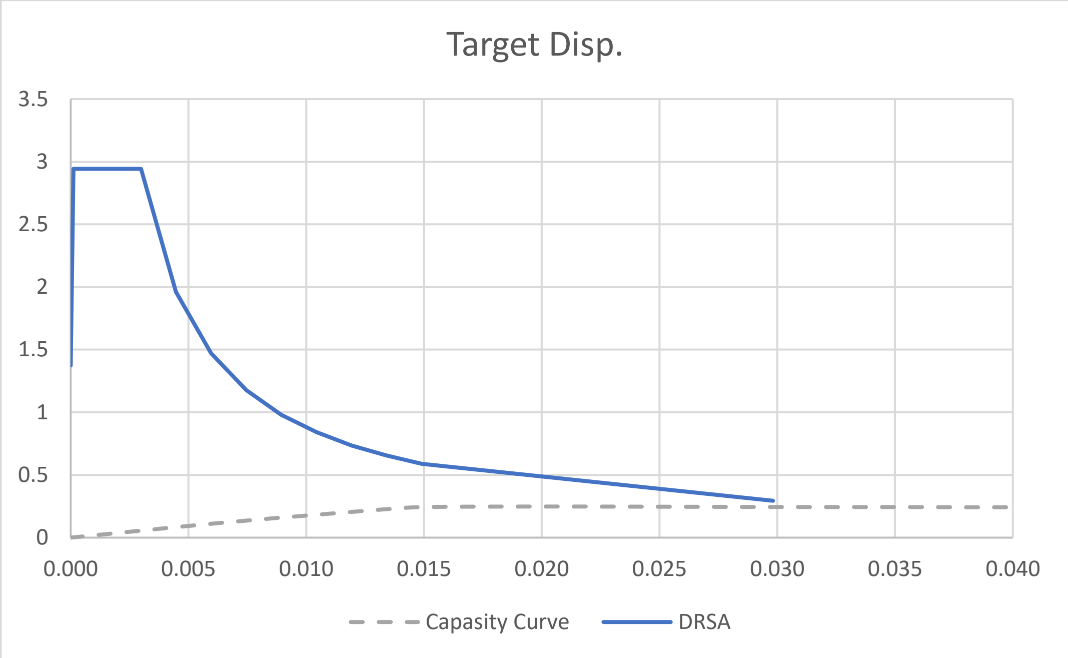

b

Figure 6.3 : Target displacement for Type 1 Building

a - 475 year b - 2475 year

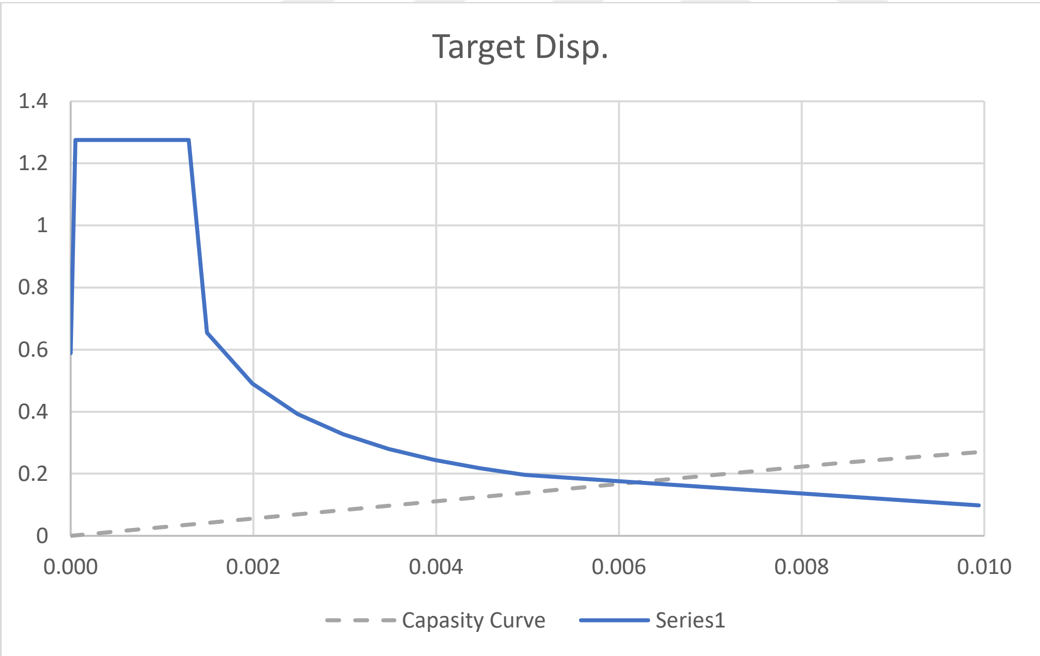

a

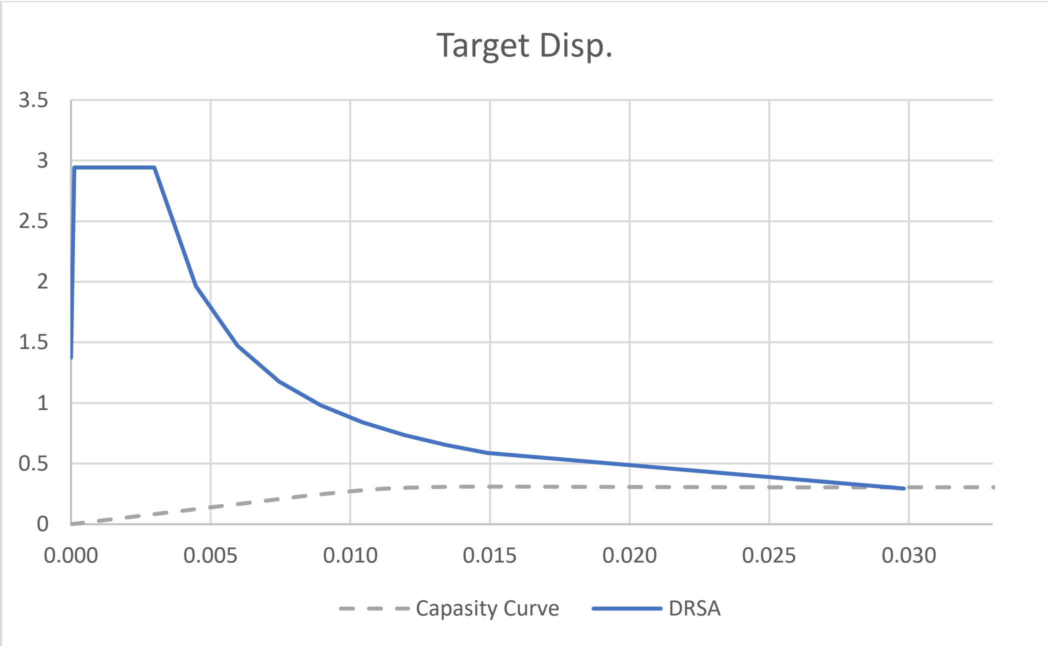

b

Figure 6.4 : target displacement for Type 2 Building

a - 475 year b - 2475 year

So the estimation of the damage of both types using fragility curve will be as following:

- **Type 1 building :** The maximum target displacement caused by earthquake as given in spectral acceleration for Misurata city is 0.008 meters for 475 year, and 0,03 meter for 2475 year. The percentage of damages of type 1 building for maximum displacement in Table 6.2.

Table 6.2 : Estimate damage of case study building (Type 1)

Damage State	Damage Percentage %	
	475 year	2475 year
Slight	30 %	70 %
Moderate	10 %	45 %
Extensive	0 %	13 %
Complete	0 %	3 %

- **Type 2 building :** The maximum target displacement caused by earthquake as given in spectral acceleration for Misurata city is 0.006 meters for 475 year, and 0,03 meter for 2475 year. The percentage of damages of type 2 building for maximum displacement in Table 6.3.

Table 6.3 : Estimate damage of case study building (Type 2)

Damage State	Damage Percentage %	
	475 year	2475 years
Slight	20 %	70 %
Moderate	7 %	45 %
Extensive	0 %	13 %
Complete	0 %	3 %

7. CONCLUSIONS

In this thesis, FEMA HAZUS loss estimation methodology were applied to find the fragility curve to determine what level of damage the building will sustain under various levels of earthquakes. The generated fragilty curves for the two types of buildings in this study are similar due to the columns are exposed to the damages prior to the beams. The basic capacity based methodoloy for earthquake design require a ductile system with strong columns and weak beams. Based on the analyses results, the current construction practice in Libya for low-rise buildings may have lack of the ductlity in the columns. Therefore, we suggest to increase the size of culomns in such type buildings in order to increase the ductlity together with using special seismic hoop reinforcements and cross ties. Also, we advise to take in consideration the minimum seismic requirment (PGA=0.1g) in designing new residential buildings for locals.

REFERENCES

Al-Heety, E.A., (2013), Seismicity and seismotectonics of Libya: as an example of intraplate environment, Arab Journal Geosci (2013), Vol 6: 9-12, Saudi Society for Geosciences, Saudi Arabia.

Suwihli, S. and Paradise, T. (2020) Creating a Libyan Earthquake Archive: From Classical Times to the Present. Open Journal of Earthquake Research, 9, 367-382. doi: 10.4236/ojer.2020.94021.

Kebeasy, R., (1980), Seismicity and seismotectonic of Libya. Salem M, Busrewill M (eds) Geology of Libya, vol 3. Academic Press, London, pp 955–963

Suleiman, A.S., Albini, P. and Migliavacca, P., (2004), A short introduction to historical earthquakes in Libya, ANNALS OF GEOPHYSICS, Vol 47: 6-8, University of Tripoli, Libya.

Hassen, H.A., (1983), SEISMICITY OF LIBYA AND RELATED PROBLEMS, Colorado State University, 25-41, USA.

FEMA (2020), Hazus Earthquake Model Technical Manual, Section 5: 1-72, USA.

Lagesse, R., Free, M. and Lubkowski, Z., (2017), PROBABILISTIC SEISMIC HAZARD ASSESSMENT FOR LIBYA, 16th World Conference on Earthquake, 1-3, Santiago Chile, Chile.

Ambraseys, N.N. (1994) Material for the Investigation of the Seismicity of Libya. Libyan Studies, 25, 7-22.

Campbell, A.S. (1968) The Barce (Al Marj) Earthquake of 1963. In: Geology and archaeology of Northern Cyrenaica, Libya, Petroleum Exploration Society, Libya, 183-195.

CURRICULUM VITAE

Name Surname : Majdi Abu Zeyan

EDUCATION :

- **B.Sc. :** 2013, Misurata University, Engineering Faculty, Civil Engineering
- **M.Sc. :** 2023, Istanbul Technical University, Engineering Faculty, Structural Engineering Department